Flexible and Wearable Acoustic Wave Technologies

*Jian Zhou[1], Yihao Guo[1], Yong Wang[2,3], Zhangbin Ji[1], Qian Zhang[2,3], Fenglin Zhuo[1], Jingting Luo[4], Ran Tao[4,3], Jin Xie[2], Julien Reboud,[5] Glen McHale,[6] Shurong Dong[7], Jikui Luo[7], Huigao Duan[1,8] *, Yongqing Fu[3,2,] **

1 College of Mechanical and Vehicle Engineering, Hunan University, Changsha 410082, China

2 The State Key Laboratory of Fluid Power and Mechatronic Systems, Zhejiang University, Hangzhou 310027, China

3 Faculty of Engineering and Environment, Northumbria University, Newcastle upon Tyne, NE1 8ST, United Kingdom

4 Shenzhen Key Laboratory of Advanced Thin Films and Applications, College of Physics and Energy, Shenzhen University, 518060 Shenzhen, China

5 Division of Biomedical Engineering, School of Engineering, University of Glasgow, Glasgow, G12 8LT, United Kingdom

6 Institute of Multiscale Thermofluids, School of Engineering, University of Edinburgh, Kings Building, Edinburgh, EH9 3FB, United Kingdom

7 College of Information Science and Electronic Engineering, Zhejiang University, Hangzhou 310027, China

8 Greater Bay Area Innovation Institute, Hunan University, Guangzhou, 511300, China.

Corresponding E-mail: duanhg@hnu.edu.cn; richard.fu@northumbria.ac.uk

Abstract: Flexible and wearable acoustic wave technology has recently attracted tremendous attention due to their wide-range applications in wearable electronics, sensing, acoustofluidics and lab-on-a-chip, attributed to its advantages such as low power consumption, small size, easy fabrication, and passive/wireless capabilities. Great effort has recently been made in technology development, fabrication, and characterization of rationally designed structures for next-generation acoustic wave based flexible electronics. Herein, advances in fundamental principles, design, fabrication, and applications of flexible and wearable acoustic wave devices are reviewed. Challenges in material selections (including both flexible substrate and

piezoelectric film) and structural designs for high-performance flexible and wearable acoustic wave devices are discussed. Recent advances in fabrication strategies, wave mode theory, working mechanisms, bending behavior and performance/evaluation are reviewed. Key applications in wearable and flexible sensors and acoustofluidics, as well as lab-on-a-chip systems are discussed. Finally, major challenges and future perspectives in this field are highlighted.

Keywords: Flexible; wearable; surface acoustic wave; piezoelectric; sensor; lab-on-chip

1. Introduction

Surface acoustic waves (SAWs) are those acoustic waves that propagate on the surfaces of the substrate, with majority of their wave energy localized on or near the surface region. SAWs are usually generated using electrodes called interdigitated transducers (IDTs), which are periodic and comb-like metallic finger structures, deposited on a piezoelectric material. When sinusoidal voltages with a period same with that of IDTs are applied, mechanical vibrations are generated from the IDTs, forming SAWs which can effectively propagate on surface of the material. SAW technologies have been widely used in radio-frequency communication such as filters[1] and frequency duplexers,[2] electro-acoustic modulator,[3] spin-based information processing,[4] Quantum control,[5] environmental gas[6] and biochemical sensing,[7] drug development,[8] healthcare,[9] medical and life sciences,[10] as well as acoustofluidics and lab-on-a-chip (LOC) applications.[11-14] They have great advantages such as low power consumption, simple structure, easy fabrication, small size, and passive/wireless capabilities. For example, AMDI company and SANDIA laboratory in the USA have recently developed a handheld rapid diagnostic screening platform using SAW sensors as the core module for COVID-19 antibody target detection.[15]

In the past decade, flexible, bendable or wearable SAW devices have received extensive attention, as they provide many new directions and novel applications compared with the conventional and rigid SAW devices. Flexible acoustic wave devices have characteristics of light weight, good biocompatibility and adjustable mechanical properties, and they could also be developed for implantable devices attributed to their great advantages of wireless passivity.[16] These flexible SAW sensors can also be applied to bodies for monitoring of health parameters such as heart rate, body temperature, blood pressure, respiration, sweat and blood components, and effectively analyze relevant data automatically and remotely for disease diagnosis and analysis. For example, flexible SAW sensors can be integrated into electronic skin.[9] By optimizing the interfaces between flexible SAW devices and biological central nervous system, they can help the artificial limb to realize various sensing functions, or can provide intelligent

and bionic tactile functions which could mimic or even surpass functions of the human skin. Furthermore, a wireless flexible piezoelectric acoustics platform is promising for underwater communication and positioning applications.

However, most of current SAW devices are made on bulk piezoelectric materials or piezoelectric films on rigid substrates such as glass or silicon wafer. Therefore, they are unsuitable for applications onto bendable or deformable surfaces, or difficult to integrate with wearable electronics. In order to be applied in bendable or wearable conditions, the conventional rigid SAW devices could be fabricated into micro- or nano-structured ones, or separated and distributed into a soft matrix using multi-sensors or fusion technology. However, this strategy requires high resolution, accuracy, and position distribution for the sensors, and is often expensive and difficult to process. [17]

At present, the common approaches for preparing flexible SAW devices are through either reducing thickness of bulk piezoelectric substrate, which becomes thin enough to achieve flexibility, or depositing piezoelectric films directly onto flexible substrates. However, there are huge challenges existed for designs, fabrication and applications of these flexible SAW devices, with some of the examples listed as follows.

- Thinning process of the bulk piezoelectric ceramic is a huge challenge. The decrease of its thickness will result in an increased surface damage layer, accumulated mechanical stresses and brittle and fragile devices.
- SAW devices often require quite thick layers of the piezoelectric film, and its thickness could be as large as 10% of the SAW wavelength. This makes device fabrication difficult due to the requirement of growing thick films.
- Most flexible substrates are amorphous, e.g., many types of polymers, hence they do not have a good match of crystal lattices with the required thin films, and thus poor adhesion is commonly seen between films and many substrates.
- There is often significant dissipation of SAW energy into the flexible substrates, especially on the polymer substrates.
- Acoustic wave properties could be dramatically changed with the reduction in the thickness of the structures, for examples, wave modes, amplitude, and frequencies.
- Various sensing and acoustofluidics behaviors could be significantly changed with the significantly reduced structure thicknesses.

There are urgently needs for a systematic review on the different aspects of design and manufacture of high-performance flexible SAW devices, which would be the key guidance for their successful applications into flexible electronics, wearable sensors, acoustofluidics and LOCs. In this paper, we discussed the recent progress for the design of flexible SAWs with

designed architectures for flexible electronics in smart wearable systems and acoustofluidics LOCs, which are briefly summarized in **Figure 1**. Advanced material selections and structural designs were firstly introduced focusing on flexible electronics or wearable devices. Design, fabrication, wave mode theory, mechanisms, and evaluations of flexible SAW devices were discussed. Key applications including temperature sensors, strain sensors, humidity sensors, ultraviolet (UV) sensors, chemical sensors, biosensors, and acoustofluidics LOC system were summarized, and their applications for monitoring human activities, body temperature, respiration, UV exposure monitoring, and health-related signs and acoustofluidics applications onto bendable and three-dimensional complex surfaces were highlighted. Finally, key challenges and future perspectives of these flexible SAW devices for applications in wearable healthcare systems and flexible acoustofluidics LOC are discussed and proposed.

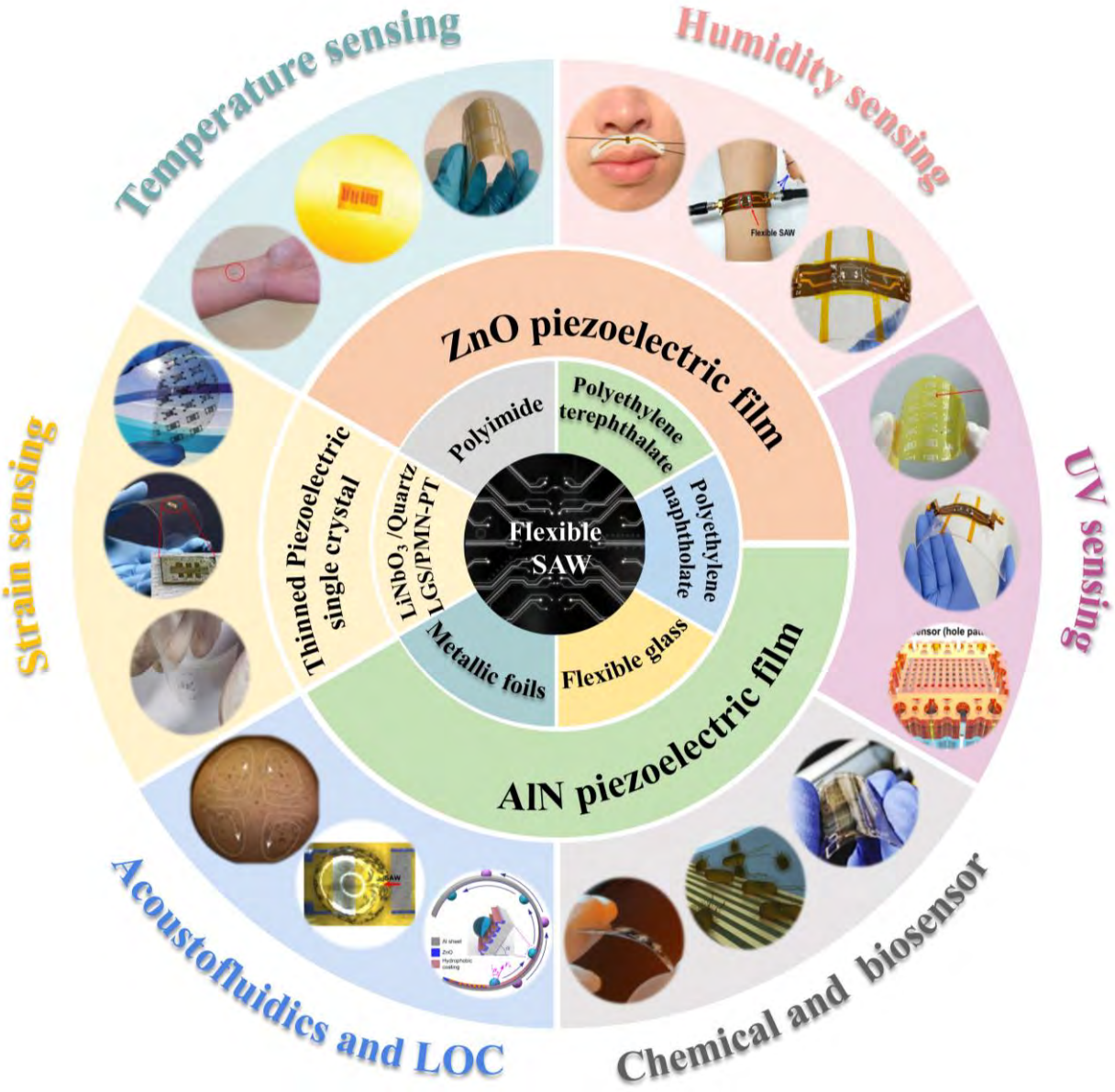

Figure.1 Flexible SAW devices substrate materials, piezoelectric film, and their application in

wearable/flexible sensors and acoustofluidics LOC. Strain sensing. Reproduced with permission from Feng et al., IEEE Sens. J. 21(17), 18571-18577 (2021). Copyright 2021 Institute of Electrical and Electronics Engineers Inc.[18] Reproduced with permission from Li et al., IEEE Elect. Device L. 40(6), 961-964 (2019). Copyright 2019 Institute of Electrical and Electronics Engineers Inc.[19] Reproduced with permission from Chen et al., J. Micromech Microeng. 25(11), 115005 (2015). Copyright 2015 IOP Publishing Ltd.[20] Temperature Sensing. Reproduced with permission from Lamanna et al., Adv. Electron. Mater. 5(6), 1900095 (2019). Copyright 2019 Wiley-VCH Verlag.[21] Humidity sensing. Reproduced with permission from Wu et al., ACS Appl. Mater. Interfaces, 12, 39817-39825 (2020). Copyright 2020 American Chemical Society.[22] Reproduced with permission from Jin et al., J. Micromech. Microeng. 27, 115006 (2017). Copyright 2017 IOP Publishing Ltd.[23] UV sensing. Reproduced with permission from Xuan et al., Procedia Engineering, 120, 364-367 (2015). Copyright 2015 Elsevier Ltd.[24] Reproduced with permission from Yin et al., Sensor Actuat. A-Phys. 15, 112590 (2021). Copyright 2021 Elsevier Ltd.[25] Reproduced with permission from Kim et al., Science, 377(6608), 859-864 (2022). Copyright 2022 American Association for the Advancement of Science.[26] Chemical and biosensor. Reproduced with permission from Lamana et al., Biosens. Bioelectron. 163, 112164 (2020). Copyright 2020 Elsevier Ltd.[27] Reproduced with permission from Piro et al., Nanomaterials, 11(6), 1479 (2021). Copyright 2021 Multidisciplinary Digital Publishing Institute.[28] Acoustofluidics and LOC. Reproduced with permission from Jin et al., Sci. Rep. 3, 2140 (2013). Copyright 2013 Springer Nature.[29] Reproduced with permission from Wang et al., ACS Appl. Mater. Interfaces, 13(14) 16978-16986 (2021).[30] Reproduced with permission from Sun et al., IEEE T. Electron Dev. 68(1), 393-398 (2020). Copyright 2020 Institute of Electrical and Electronics Engineers Inc.[31]

2. Key Toolbox for Flexible Surface Acoustic Wave Technology

In general, a SAW device consists of three major components, i.e., electrode (e.g., IDTs), piezoelectric material, and/or the substrate. All these should be configured into a hybridized system to achieve requirements of flexible SAW devices. To develop next-generation soft and ultra-lightweight wearable devices, new materials and processes must be studied. Herein, we discuss recent development of materials for flexible SAWs, including flexible substrate materials and piezoelectric materials, whereas the electrodes or IDTs are commonly used thin film metals such as aluminum or gold. The focus is on their suitability and functionality for wearable sensors and microfluidics, and key problems/ potential solutions.

2.1 Flexible Substrate Materials

Substrate often plays critical roles for achieving flexibility, user comfortability, and capacity for designability and miniaturization. Among different components of SAW devices, the substrate governs many key properties, including mechanical robustness and flexibility,

electronic performance, electrical/heat resistance or thermal stability, surface smoothness, biocompatibility, wettability, permeability, cost, and optical transparency. Following are the key special requirements for the flexible substrates.

(1) **Thermal and thermomechanical properties**. It is crucial for the compatibility of substrate working temperature, such as the glass transition temperature (T_g) of a polymer, with the process temperature. Large differences between thermal properties of the substrate and piezoelectric films often result in cracking or peeling-off issues during device's fabrication or thermal cycling.

(2) **Surface roughness**. The surface roughness of the substrate will significantly influence the physical/electrical properties of the following deposited film, device fabrication and device performance. Low surface roughness or smoothness is commonly a prerequisite for avoiding shorting in the layered electronic structures.

(3) **Mechanical properties**. Elastic modulus determines the deformation resistance of materials. A low elastic modulus makes the substrate easily bent, and a hard surface supports the rigidity of structure and maintains the device layers under deformation.

(4) **Chemical properties**. It is required that the substrates will not induce any contaminants in processes. They also need to be inert against chemical etching during processing. They should also have good barrier properties against permeation by atmospheric gases, oxygen and water.

(5) **Other functional properties**. For example, in applications which are related to the optics or photonics, good transmission and transparency, or light modulation properties are needed for the substrate materials.

At present, the main flexible and bendable substrate materials are flexible silicon, flexible polymers such as polyimide (PI), polyethylene terephthalate (PET), polyethylene naphtholate (PEN) films, flexible thin metal sheet/foils, and flexible glass, with some of the examples shown in **Figure 2 a~f**.

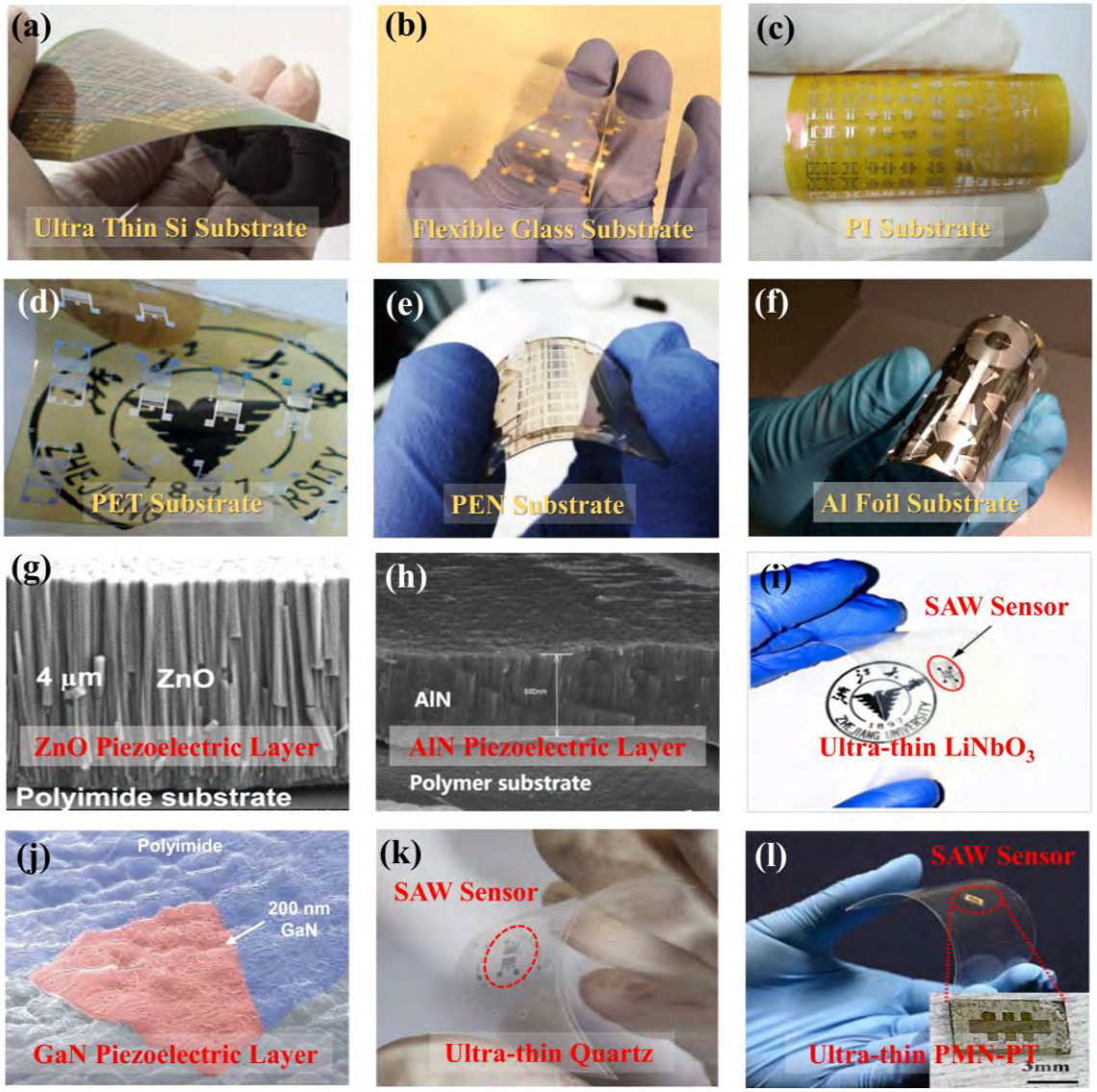

Figure2. Flexible SAW devices on different substrates and piezoelectric thin film material. (a) Ultra-thin Si substrate; Reproduced with permission from Zhang et al., Chinese. Phys. Lett. 30, 077701 (2013). Copyright 2013 IOP Publishing Ltd.[32] (b) Flexible glass substrate; Reproduced with permission from Ji et al., Microsyst. Nanoeng. 7, 97 (2021). Copyright 2021 Springer Nature.[33] (c) PI flexible substrate; Reproduced with permission from Jin et al., Sci. Rep. 3, 2140 (2013). Copyright 2013 Springer Nature.[29] (d) PET Substrate; Reproduced with permission from He et al., Appl. Phys. Lett. 104, 213504 (2014). Copyright 2014 American Institute of Physics.[34] (e) PEN substrate; Reproduced with permission from Lamana et al., Biosens. Bioelectron. 163, 112164 (2020). Copyright 2020 Elsevier Ltd.[27] (f) Al foil substrate; Reproduced with permission from Fu et al., Prog. Mater. Sci. 89, 31-91 (2017). Copyright 2017 Elsevier Ltd.[35] (g) SEM image of ZnO piezoelectric film; Reproduced with permission from Zhou et al., J. Appl. Phys. 114(4), 044502 (2013). Copyright 2013 American Institute of Physics.[36] (h) SEM image of AlN piezoelectric film; Reproduced with permission from Jin et al., Thin Solid Films. 520(15), 1863- 4870 (2012). Copyright 2012 Elsevier Ltd.[37] (i) Ultra -thin $LiNbO_3$; Reproduced with permission

from Xu et al., Appl. Phys. Lett. 122, 093502 (2018). Copyright 2018 American Institute of Physics.[38] (j) SEM image of GaN piezoelectric film; Reproduced with permission from Kim et al., Science, 377(6608), 859-864 (2022). Copyright 2022 American Association for the Advancement of Science.[26] (k) Ultra-thin Quartz; Reproduced with permission from Feng et al., IEEE Sens. J. 21(17), 18571-18577 (2021). Copyright 2021 Institute of Electrical and Electronics Engineers Inc.[18] (l) Ultra-thin PMN-PT. Reproduced with permission from Li et al., IEEE Elect. Device L. 40(6), 961-964 (2019). Copyright 2019 Institute of Electrical and Electronics Engineers Inc.[19]

2.1.1 Thin Silicon Substrates

Previous studies to achieve good flexibility of SAW devices were focused on reducing the thickness of single crystal silicon, which becomes quite flexible as shown in **Figure 2a**. For example, Zhang et al. proposed a strategy to apply flexible acoustic wave devices based on flexible AlN/Si structure (on a 50 μm thick silicon), which exhibited a large bending radius of curvature (8 mm).[32] However, the process of thinning silicon is relatively difficult and expensive, and devices are brittle and fragile, attributed to the brittleness of silicon substrate. Some of the key properties for flexible thin silicon are highlighted in **Table 1.**

2.1.2 Flexible Glass

Flexible glass (**Figure 2b**) is a term used for glass substrates with a thickness below 200 μm. Within this thickness range, the glass exhibits good bendability and flexibility similar to those of plastics or metal foil substrates.[39] Flexible glass retains all the advantages of the bulk glass, e.g., an large optical transmittance (larger than 90% in visible light), a low stress birefringence, a smooth surface with a good temperature tolerance (up to 600 °C), a root mean square (RMS) roughness of 1 nm or less, a low coefficient of thermal expansion (CTE, ~4×10^{-6}/°C), a high dimensional stability, a good resistance to chemical processes, a good scratch resistance and electrical insulation, and a good impermeability against oxygen and water. Chen et al. fabricated flexible/transparent ZnO thin film SAW devices on ultrathin flexible glass substrates.[16] Indium tin oxide (ITO) electrodes have also been used onto ZnO/glass to form a fully transparent and flexible device. These glass-based flexible acoustic wave devices showed similar performance in comparisons with those of rigid glass ones, with much better optical transmittance. Highly sensitive strain and humidity sensing were demonstrated using this flexible glass SAW devices.[20,33,40] Compared with other SAW devices fabricated on flexible substrates such as polymer materials, the SAW devices based on flexible glass represents good mechanical and chemical properties, as well as low loss of wave propagation. Some of the key properties for flexible glass are highlighted in **Table 1**.

However, it should be addressed that flexible glass is quite fragile and thus difficult to

handle. To solve this issue, following measures can be taken during processing, e.g., (1) laminating with plastic foils; or (2) coating with a thick polymer layer. [41,42]

2.1.3 Polymers

Polymer substrates are normally highly flexible and inexpensive, with the good capability for roll-to-roll processing. The mostly commonly used flexible polymers in organic electronics are the polyesters, such as PI, PET and PEN (**Figures 2c-e**). **Table 1** compares the key properties of these polymer materials. In 2013, Jin et al. reported flexible SAW sensors by depositing piezoelectric ZnO films on PI substrate, demonstrating excellent temperature sensing capability.[29] After that, various flexible SAW sensors including strain sensor,[38] humidity sensor, respiration monitoring sensor,[43] UV sensor,[44] and microfluidics[45] have been reported using various types of polymer substrates such as PI, PET and PEN. In 2020, Tao et al applied polymer as a transition layer to fabricate polyimide-coated woven carbon fibers based flexible SAW devices, integrating electromagnetic metamaterials and ZnO/PI SAW sensors, demonstrating their capabilities of wireless, *in situ*, noninvasive, and continuous detecting of various environmental parameters and biomolecules.[46] Those PI substrates are quite flexible, but often show poor strain sensitivity and transparency.

Commercial PET films have also been used as the substrates to develop the bendable SAW devices, due to their good flexibility, high transparency, reasonably thermal and chemical stabilities, as well as low cost.[34] In 2014, He et al. used highly vertically aligned ZnO films on PET substrates, and the fabricated SAW devices performed well even after repeated flexion up to 2500 με for 100 times.[34] In 2018, Xu et al. reported to bond the PET film with a polished thin layer of $LiNbO_3$ film (58 μm) for fabrication of flexible SAW devices to prevent the wafer from breaking.[38]

PI has a limited optical transmittance in visible/IR light wavelength range, therefore, a flexible thermoplastic polymeric material such as PEN was applied as the substrate for flexible SAW devices, due to its thermal and chemical stability, biocompatibility, and transparency in the visible spectral range.[46] In 2020, Leonardo et al. fabricated AlN/PEN SAW temperature sensors with a frequency in GHz, because of low-cost, bendability, disposability, flexibility, good mechanical/electrical properties, and chemical stability of the PEN. [27]

However, there are quite many challenges for these polymer substrates, with some of key issues highlighted below.

- There is significant dissipation of acoustic wave energy in polymer substrate. Polymer organic substrates will easily absorb acoustic energies, making the device to have high transmission losses. Therefore, huge challenges are existed to use them for microfluidics

or lab-on-a-chip applications. To solve this issue, Zahertar et al. reported that adding an intermediate trimetal layer (e.g., Ni/Cu/Ni) onto the polymer substrate enhanced the acoustofluidics effects.[47]

- These polymers have poor temperature tolerance/thermal stability. The low T_g of the polymer substrate limits its ability to use high temperature manufacturing processes and work at high temperatures or in a harsh environment.
- Poor dimensional stability and high values of coefficient of thermal expansion (CTE) are also issues for polymers. Most of the polymer films are dramatically shrunken during heating and cooling cycles.[48] Thermal mismatch induced stress can easily cause the free-standing devices bent dramatically. A large CTE mismatch between polymers and other materials when applied with thermal energy during processing can easily damage the device.[49]
- Many polymer substrates are amorphous, and consequently they do not provide a good match for the lattice of the required thin films, thus often causing poor adhesion between films and the substrates. The deposited piezoelectric film is often prone to cracking under a large deformation or repeated bending processes.

Table 1 Properties of Common flexible substrates suitable for flexible SAWs [50-53]

Substrate	**PI**	**PET**	**PEN**	**Flexible glass**	**Thin Silicon**	**Al foil**
Glass transition temp. (T_g)	155-360	70-110	120-155	-	-	-
Melting temperature (T_m)	250-452	115-258	269	600	1410	660
Coefficient of thermal expansion (CTE) (ppm °C^{-1})	8-20	15-33	20	3.2	5	23.21
Water adsorption (%)	1.3-3	0.4-0.6	0.3-0.4	-	-	-
Solvent resistance	Good	Good	Good	Good	Good	Fair
Transparency	Poor	Good	Good	Good	Poor	Poor
Dimensional stability	Fair	Good	Good	Good	Good	Good
Surface roughness (nm)	30	30	15	<0.5	<0.5	Poor

2.1.4. Metallic Foils

Metal foil substrates less than a few hundreds of microns thick are often quite flexible (**Figure 2f**) and have been the attractive substrates for emissive or reflective devices, although they are not transparent substrates. Compared with those polymer substrates, low-cost and widely commercially metal foil (such as Al, nickel layer) have less dissipation of sound waves and energy, thus suitable for microfluidics and lab-on-a-chip applications.[30]In addition, metal foils such as Al foil-based flexible SAW device commonly have large temperature coefficients of frequency (TCF), for example, up to -760 ppm/K, which could be explored for highly

sensitive temperature sensing applications. However, metal foil as a substrate for flexible SAW devices do have the following key challenges.

- Metal foils usually show certain amount of permanent plastic deformation, and often not recovered to their original shapes after bending.
- Metal foils generally have rolling patterns or micrometer-size inclusions, with a high surface roughness typically ~100 nm RMS, much larger than that of a standard thin glass (commonly less than 1nm RMS). This makes it very difficult to fabricate high frequency devices (or micron or sub-micron SAW wavelengths) on metal foil.
- To ensure electrical insulating and acoustic wave properties of the thin film SAW devices made on these metallic foils, they often need either well-polished or coated with film layers.
- Metal foil is easy to tear or become crumpled. These metallic foils often show defects if permanently deformed patterns or not handled well.
- Many metal foils are incompatible with microelectronic processes and could introduce impurity ions, even though they can be applied in roll-to-roll and mass production processes.

2.2 Piezoelectric Thin Films

Most of the above substrates are not piezoelectric, therefore, a piezoelectric thin film is commonly needed to realize an acoustic wave device. Acoustic wave technologies based on piezoelectric thin films such as ZnO, AlN and PZT[54,55] have been commonly applied for sensing and acoustofluidics/LOC applications[56,57]. Gallium nitride (GaN), $LiNbO_3$, and poly (vinylidene fluoride) or PVDF are other commonly investigated piezoelectric materials. **Table 2** summarizes and compares the properties of several piezoelectric materials including many types of thin films. In the following sections, major types of piezoelectric films are discussed.

2.2.1. ZnO Piezoelectric Film

Zinc oxide (ZnO) film is attractive for photonics, electronics, piezoelectrics, and optoelectronics devices, acoustics and sensors,[58,59] and high crystallinity of films can be easily achieved without applying substrate heating in deposition[60] as shown in **Figure 2g**. It normally shows low stresses and good adhesion on many substrates such as glass and polymers. Films with thicknesses of tens of microns can be easily obtained. Hence, it is very suitable for SAW devices with a thick layer required or acoustic wave devices operated at a much lower frequency range.[61]

ZnO piezoelectric film was firstly reported for applying into flexible SAW device using the magnetron sputtering method[29]. ZnO thin films are widely used in SAW based temperature, strain sensor, gas-sensing devices, and ultraviolet detectors, because of its low cost, safety, good piezoelectric properties and both optical and electrical properties. In addition, ZnO is

hydrophilic, which means water molecules are easily absorbed on surface of ZnO device with a relatively higher humidity. This causes mass loading effect on the device's surface, resulting in the changes of its transmission characteristics, which can be explored for high sensitivity SAW humidity sensors[62].

Deposition conditions, crystal quality and thickness of films affect the properties of ZnO based flexible SAW devices. In 2013, Zhou et al. studied reported that the optimized deposition conditions and relative larger thickness of ZnO will lead to better film quality and improved performance of SAW devices. [36] Liu et al. explored ZnO/Al foil SAW devices for flexible acoustofluidics,[63] and also reported similar studies for ZnO/Al foil based flexible SAW.[64]

Another competitiveness of ZnO is that its nanostructures and nanowires can be easily prepared on these devices, which have been intensively explored for various sensing and detection applications.[22,25]

Some of the key properties for ZnO are highlighted in **Table 2.** However, there are still many issues related to the ZnO films. For example, the strong reactivity and chemical instability of ZnO is troublesome for biomedical applications (unless using surface protection or packaging methods).[35] ZnO could become unstable when exposed to high humidity conditions, or put into water for quite a long time, which poses issues of stability and reliability. ZnO also shows large dielectric losses and instable at high temperatures (for example, above 500 °C). Finally, Zn is a contaminant for integrated circuit (IC) or complementary metal oxide-semiconductor (CMOS) processes.

2.2.2. AlN Piezoelectric Film

Aluminum nitride (AlN) is a III-V and broadband gap semiconductor material, and its forbidden bandwidth is 6.2 eV at room temperature. It has a high Rayleigh acoustic velocity of 5760 ms^{-1}, and thus suitable for GHz-level SAW devices, which could have great potentials in 5G wireless communication system and high precision sensing.[65] It has good compatibility with CMOS and microelectronics technologies. It can be deposited by physical vapor deposition at low temperatures (e.g., from room temperature and up to 400°C). AlN based SAW devices shows a better chemical stability in acid–alkali conditions, if compared with ZnO films, and it is more suitable for harsh environment.[66]

In 2012, Jin et al. investigated crystalline structures of AlN films on flexible PI deposited using a reactive sputtering method, as shown in **Figure 2h**.[37] They further fabricated AlN-based flexible SAW devices on PI substrate, with lamb waves and acoustic wave velocities up to 9000~10000 m/s.[67] Lamanna et al. fabricated flexible and transparent AlN-based SAW devices on a PEN substrate using sputtering deposition. A large transmission-signal amplitude, up to

~20 dB, was achieved for the Lamb mode SAWs with an acoustic velocity of ~10,500 m s^{-1}. They found that compared to those on a silicon substrate, the AlN/PEN flexible SAW device shows a better performance of flexible, and a TCF value as high as ~-810 ppm/°C. They also demonstrated flexible AlN SAW based temperature sensor, strain sensor, photo-response detector, wearable pH sensors and flexible biosensor on the PEN substrate.[27] In 2021, Li et al deposited highly oriented (0002) AlN films with a low roughness of 3.2 nm, and the SAW device showed a piezoelectric coefficient d_{33} of ~8.01 pm/V.[57] The device has a center frequency up to ~4.95 GHz, and its piezoelectric and frequency characteristics can be maintained up to 10,000 bending cycles.[68] Some of the key properties for AlN films are highlighted in **Table 2.**

However, deposition of AlN films and their texture control are more difficult than those for ZnO films.[69] For examples, oxygen or moisture in the deposition chambers and substrate orientation have significant effects on growth and microstructures of AlN films. It is a challenge to deposit AlN films of a few microns thick, due to large film stress and formation of cracks. Therefore, AlN film is more applicable for operation with a high frequency, which often requires a very thin piezoelectric film. Whereas for ZnO film, it could be more suitable for devices operated with lower frequencies which might require a thicker piezoelectric film. Finally, nanowires of AlN have not been frequently reported.[35]

2.2.3 PVDF Films

Poly (vinylidene fluoride) (PVDF) has outstanding properties among polymers, including thermal stability, good mechanical strength, high hydrophobicity, and chemical resistance.[70] It is an intrinsic flexible polymer with good piezoelectricity. It is a semicrystalline polymer with four different phases. However, only one of which, namely β phase, shows spontaneous polarization phenomenon and the piezoelectricity.[71] In addition, it is creep resistant, relatively tough, and chemically inert. It has also good stability when exposed to sunlight, compared to other types of piezopolymers.[72,73]

There are many reports of PVDF being used for interdigital transducers. In 1997, PVDF transducer with the Lamb waves was reported.[74] In 2007, Preethichandra et al. investigated to apply PVDF for a bending sensor. Their experimental results showed that when the PVDF substrate was bent, the PVDF sensor responded well to the bending curvatures, and its amplitude and phase angle were varied with the variation of curvatures.[75]

Some of the key properties for PVDF are highlighted in **Table 2.** However, PVDF has several inherent disadvantages which limit its usages, including its low values of d_{33} and d_h. The PVDF film also requires a large level of electric field for post-poling process, which is

quite difficult to process. In addition, it cannot be used at high temperatures (e.g., above 150 ^{o}C), which make its applications for many conditions difficult. Finally, the PVDF is a soft material, and it has large dissipations of sound waves and energy.

2.2.4 Lithium Niobate Film

$LiNbO_3$ is pivotal for acoustic technology, due to its large electromechanical coupling coefficient, and relatively low cost due to mass production. It is desirable if $LiNbO_3$ can be prepared into a thin film format, which not only maintains its large electromechanical coupling coefficient, but also improves its sound velocity or flexibility.

Sputtering is the earliest proposed method to grow $LiNbO_3$ thin films, but the method was often reported to produce films with poor crystal quality, thereby causing their high propagation losses.[76] Many studies[77-82] showed that there is a critical issue of lithium deficient in the $LiNbO_3$ films sputtered from a stoichiometric target, and thus a Li-rich target or a secondary lithium target source must be used to compensate this lithium deficiency.

One of the recent advances for making high quality SAW devices is based on the transferring of lithium niobate crystals (**Figure 2i**). Using transferring techniques such as crystal ion slicing[83] and grinding, single crystalline $LiNbO_3$ films were fabricated and showed good properties, uniformity, and low defect density.[84] They can be directly bonded onto the SiC or Si substrate to generate high performance and achieve a high acoustic velocity (or high resonant frequency). For example, Zhang et al. reported single-crystalline X-cut $LiNbO_3$ films on a 4H-SiC substrate, which were prepared using ion-slicing and wafer-bonding processes. The obtained resonator showed a large k^2 of 26.9 % and a high-quality factor of 1228 at 2.28 GHz.[85] This single crystal based thin films can also offer remarkable flexibility than those of bulk counterparts. Xu et al. developed flexible SAW sensors made on single crystalline 128°Y-cut $LiNbO_3$ film fabricated by grinding/polishing technique of bulk crystals.[38] Floer et al. achieved interrogated and wireless sensing functions up to 25 cm, after optimizing the antenna designs and impedance matching between the antenna and the thinned single crystalline $LiNbO_3$ SAW sensor.[86]

Some of the key properties for $LiNbO_3$ film are highlighted in **Table 2.** With the development of information and communication technology, thin film of single crystalline $LiNbO_3$ are crucial in the miniaturization, flexible, high-frequency of SAW devices, and integrated into CMOS or microelectronics, but deposition of high-quality $LiNbO_3$ single crystal films is still a challenge. [76] One of the best methods is the ion implantation which can uniformly damage and thus slice thin layers of $LiNbO_3$, often called ion-sliced technology, is currently the preferred method. However, it requires a minimum thickness of 300 nm for bonding with

a wafer followed by transferring thin film. It is often limited to a few microns because of limited applied implant energies. It thus has many straggle-related damage and thus needs post-treatment for polishing and thermal annealing to improve its optoelectrical properties.[87] Although single crystal $LiNbO_3$ thin film can provide significant flexibility, the devices manufactured are often brittle and fragile.

2.2.5 Other Types of Piezoelectric Thin Films

GaN is an n-type and direct band gap semiconductor material with a band gap width of 3.39 eV. GaN has high thermal conductivity, high hardness, high melting point and high thermochemical stability. Kim et al.[9] reported a chip-less and wireless e-skins based on SAW sensors made of freestanding single crystalline piezoelectric GaN film (**Figure 2j**), which offered a highly sensitive, low-power, and long-term sensing of strain, UV, and ion concentrations in sweat. Due to the high temperature required for GaN growth, it is impossible to grow GaN on flexible substrates directly. Therefore, the transfer method has become the main-stream technology of flexible GaN devices. However, the transfer process easily leads to interfacial and material damages. The low thermal conductivity of the flexible substrate leads to difficulty in heat dissipation. Output power of the flexible GaN RF power devices is quite low at present. All of these issues limit their application and development in the field of flexible electronics.

PZT has the largest electromechanical coupling coefficient and piezoelectric constant among all piezoelectric film materials. However, it has its disadvantages as biosensors due to their low-quality factor, low acoustic wave velocity, and poor biocompatibility (mainly due to the toxicity of Pb). Fabrication of thick PZT film is also a challenge for making SAW devices. The frequently required high electric field polarization process and high temperature annealing procedure if using a sol-gel method cause its unsuitability for integration with CMOS and microelectronic processes.

Quartz has relatively poor piezoelectric properties, but it is widely used to fabricate SAW devices due to its shear-horizontal wave generation, high quality factor, and a low TCF value. Some of the key properties for Quartz are highlighted in **Table 2.** Ultra-thin AT-X quartz (**Figure 2k**) of 64 μm thick is commonly used for fabricating high-frequency resonators, and it can be thinned further to about 31 μm using inductively coupled plasma (ICP) deep reactive ion etching (DRIE) process, to fabricate flexible SAW with Q factor high up to 781, and a TCF of −1.06 ppm/◦C.[18]

Single-crystalline (72%) Pb(Mg1/3Nb2/3)O3- (28%)PbTiO3 (or called PMN-PT) ceramic is also a good choice due to the large piezoelectric constant d_{33}, which can reach up to

2000 pC/N and be 4~6 times of PZT-4 piezoelectric ceramic. In 2019, Li et al. reported SAW devices which employ the piezoelectric single crystal PMN-PT thick film onto a stainless-steel flexible substrate (**Figure 2l**). The bulk PMN-PT is thinned down to about 37 μm by chemical-mechanical process method and the SAW device can achieve a high sensitivity of strain measurement over a range from -1000 to +1000 με.[19]

Langasite (LGS), a good candidate for high-temperature SAW sensors, shows excellent piezoelectric properties at high temperatures above 1000°C. Zhang et al. fabricated a SAW device based on ultra-thin LGS, by grinding and polishing the bulk LGS to 100 μm using chemical mechanical polishing method. This material could achieve flexible and bending acoustic wave functions at a high temperature of 500°C.

However, the thinning process used to achieve the above film structures impacts their mechanical properties. During thinning using grinding method, the sub-surface damage and cracks generated in SAW devices result in poor bendability and eventually lead to early breakage of devices.[88] Most ultra-thin piezoelectric crystals reported at present were obtained by grinding the block material, which requires strict processing technology. In actual production, the film thickness of materials cannot be accurately controlled, and the uniformity of grinding cannot be guaranteed to be completely uniform. Damage in the sub-layers induces large stresses in the much thinned wafer, which causes warping of thin wafers.[88]

Table 2 Comparison of common piezoelectric materials.[35]

Properties	**ZnO**	**AlN**	**PZT**	**PVDF**	**128°Cut LN**	**Quartz**
Density (10^3kg/m^3)	5.61-5.72	3.25-3.3	7.57	1.78	4.64	2.64
Modulus (GPa)	110-140	300-350	61	2.5	130-170	71.7
Refractive index	1.9-2.0	1.96	2.40	1.42	2.29	1.46
Piezo-constant d_{33}(pc/N)	12	1.5,6.4	289-380,117	-35	19-27	2.3(d11)
Effective coupling coefficient, k^2 (%)	0.15-0.28,0.33 1.5-1.7	0.17-0.5 3.1-8	0.49 20-35	0.12-0.2 2.9	0.23 2-11.3	0.0014 0.004
acoustic velocity (*m/s*)	6350	10400	4000~6000	1500~2200	3680~3980	5960 (3310)
TCF / ($\times 10^{-6} \cdot ℃^{-1}$)	-60	-25	+80	~	-85	0
Inherent material loss	low	Very low	high	~	low	low
acoustic impedance	low	high	low	low	low	low
Bandwidth	narrow	narrow	wide	wide	narrow	narrow
production costs	low	high	Very high	low	low	low
CMOS compatible	incompatible	compatible	incompatible	~	compatible	Compatible
Main applications	SAW filter, SAW	FBAR, SAW	Piezoelectric sensor	Medical Electronics	SAW Sensor	TC-SAW QCM

3. Advances in Theoretical and Fundamental Aspects of Flexible Acoustic Waves Devices

Flexible SAW devices based on the above substrates or piezoelectric films[18,19,38] can be theoretical analyzed using the methods similar as those for the conventional SAW devices based on bulk materials.[89,90] In this section, we will focus on the novel layered structure based flexible SAW and discuss the fundamental issues including film thickness effects, acoustic wave mode evolution, bending deformation including elastic and non-uniform elastoplastic deformation behaviors of thin film flexible SAW devices.

3.1 Film/Substrate Thickness Effects

Thin film based acoustic wave devices usually exhibit significant dispersion effects, which means that their resonant frequency, wave velocity, electro-mechanical coupling coefficient, and quality factors are highly dependent on piezoelectric film thickness[91]. The film thickness-to-wavelength ratio and the normalized film thickness (*hk*, where *h* is film thickness and *k* is wave vector, k= 2π/λ) determine wave modes and their velocities.[35] Acoustic waves mainly propagate in the piezoelectric film if its thickness is greater than or equal to the SAW wavelength λ. In this case, wave velocity will be near to that of Rayleigh waves (e.g., ~5600 m/s for AlN and ~2800 m/s for ZnO). If the thickness of piezoelectric films is much smaller than the wavelength, most of the wave energy is concentrated within the substrate.

Thickness of ZnO film on wave transmission properties for ZnO/polyimide SAW devices was reported by Zhou et al. [36] With the increase in ZnO film thickness, both the resonant frequency (f_0) and transmission signal amplitude (S_{21}) of the SAW devices increase with the thickness of ZnO film as shown in **Figures 3a&b**. This is mainly due to the enhanced piezoelectric effect and the increased grain sizes, thus the resulted increased acoustic wave velocity of ZnO films (2700 m/s) compared with the that of the polymer substrate (700 m/s)[36]. They compared resonant frequencies and phase velocities from both simulations and experiments with good agreements. When the ZnO film is thin, phase velocity of the SAW is mainly attributed to that of polyimides. However, with the increased thickness of ZnO film, wave velocity reaches ~70% of the single crystal ZnO.

For flexible substrates, the wavelength, λ, is commonly much larger than thickness of the substrate, *H*. Wave modes in these acoustic wave devices are often not pure Rayleigh wave modes, but Lamb waves, especially when the wavelength λ is much larger than the thickness of the whole devices. Lamb mode are often generated on thin films with only piezoelectric films. Tao and wang et al. found that the thickness of the substrate plays an important role in

the selection of wave modes.[30,92] When the thickness of the substrate is larger than the wavelength, e.g., $\lambda/H < 1$, Rayleigh mode is dominant. If $\lambda/H > 1$, Lamb mode is dominant. However, mixed mode (Rayleigh and Lamb) is usually observed $\lambda/H = 1$, as shown in **Figures 3c-f**.

3.2 Evolutions of Acoustic Wave Modes

Most of SAW devices are using their Rayleigh mode, and many of them have higher modes of Rayleigh waves, such as Sezawa modes in the layered SAW devices. The Sezawa mode is a guided wave generated when the acoustic velocity of the piezoelectric film layer is much lower compared to the substrate or sub-layer beneath. The acoustic waves generated in a thin film/substrate device propagate along the interface with a much higher velocity than that of the top piezoelectric film layer[93]. Rayleigh mode devices often show substantially vertical displacements and rapidly dissipates its energy into the liquid on the surface. Therefore, for sensing applications in liquid, this will lead to excessive damping, thus they are not suitable for sensing in liquid or highly humid conditions. Shear horizontal SAWs (SH-SAWs) or surface transverse waves (STWs) are ideal for *in situ* or real-time sensing in a liquid medium because they propagate along the surface within a horizontal plane and do not significantly dissipate their wave energy into the liquid,[94,95] suitable for *in situ* or real-time sensing in a liquid medium. Therefore, for flexible or wearable applications, the waves modes between Rayleigh and SH-SAW, or even STW should be selected or designed for various situations.

Both the Rayleigh waves and Lamb waves were commonly observed for the acoustic wave devices of ZnO/PI, ZnO/ PET, ZnO/Al foil, AlN/flexible glass, and AlN/PEN.[35] Lamb waves are commonly produced if the substrate's thickness is much smaller than or comparable to the wavelength. There are two common Lamb wave modes when they propagate in a thin plate or a membrane, zero-order antisymmetric mode, A_0,[96] symmetrical Lamb wave mode or extensional mode, S_0. Compared with that of A0 mode, the S_0 wave mode has much less energy dissipated into the liquid, and thus is suitable for sensing in the liquid environment. In contrast, the Lamb waves travel within the whole plate, less influenced by the substrate's mechanical property changes.[21]

The excited modes of Rayleigh or Lamb ones can be changed with different thicknesses of substrate or films and also the wavelength of the waves. Tao et al reported that for the ZnO/Al foil device, when the thickness of the Al substrate is increased at the same wavelength, the wave modes of the devices are changed from Lamb waves to Rayleigh waves.[97] For example, when the wavelength is 160 μm, wave mode for in Al foil of 50 μm thick shows Lamb waves including both A0 and S0 modes (**Figure**. **3g**). These Lamb waves are excited because the

thickness of piezoelectric film and substrate is much lower than that of the wavelength. With the increase of Al thickness, for example, for a device made on a 200 μm thick Al plate, a Rayleigh-Lamb hybrid wave can be obtained with the same wavelength of 160 μm. When the thickness of Al plate is increased to 600 μm and 1.6 mm, the Rayleigh and its higher Sezawa modes are dominant.

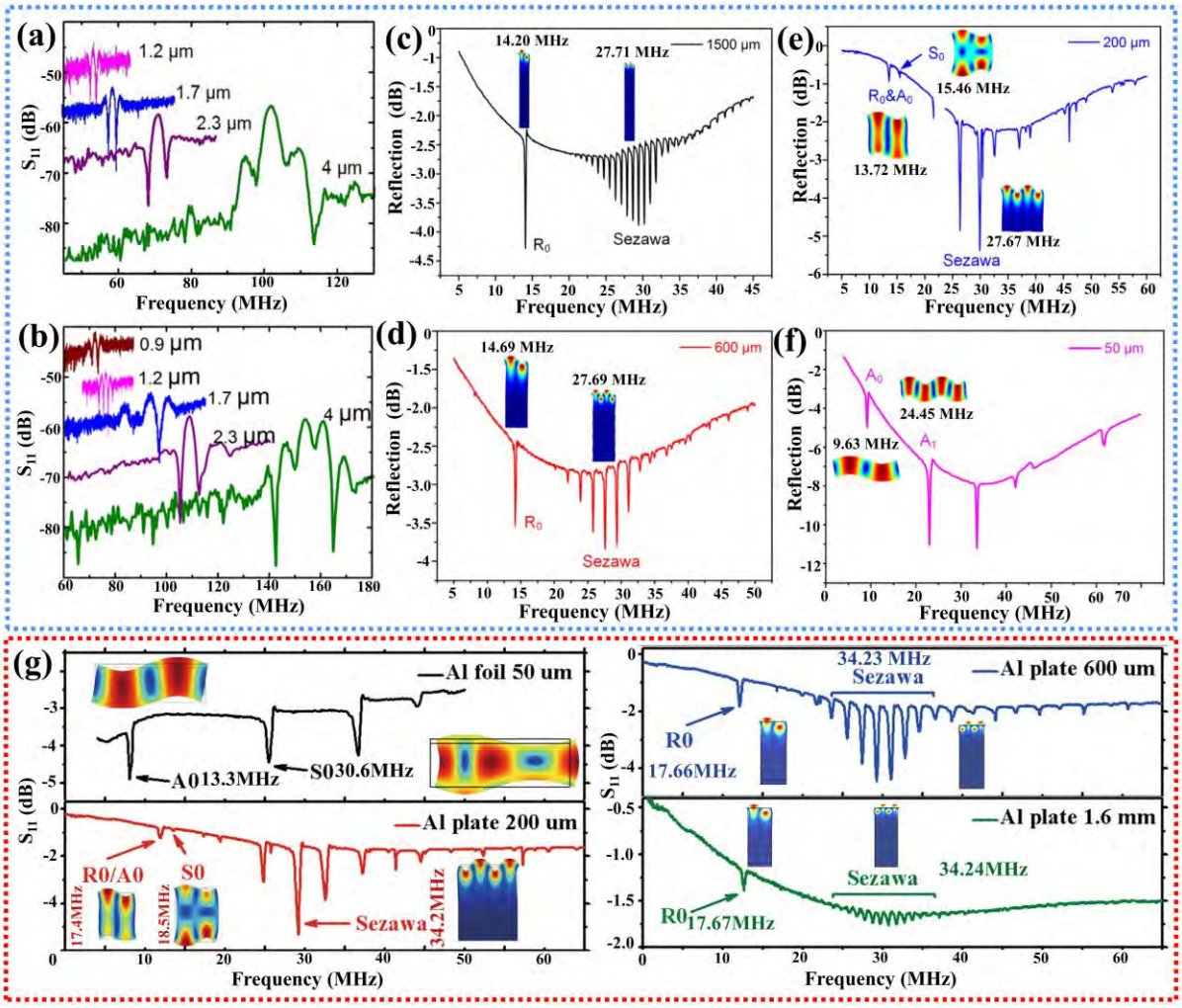

Figure3. The influences of film/substrate dimensions on the resonant frequency of flexible SAW devices;(a) and (b) The effects of the ZnO piezoelectric layer thickness on the resonant spectra of the flexible SAW devices, with wavelengths of 16 μm and 12 μm; Reproduced with permission from Zhou et al., J. Appl. Phys. 114(4), 044502 (2013). Copyright 2013 American Institute of Physics.[36] (c-f) The reflection spectra of ZnO/Al SAW devices with a wavelength of 64 μm. FEA simulation and experiments verified the wave vibration modes and resonant frequencies for the SAW devices with a wavelength of 200 μm and Al sheet thicknesses of (c) 1500, (d) 600, (e) 200, and (f) 50 μm; Reproduced with permission from Wang et al., ACS Appl. Mater. Interfaces 13(14) 16978-16986 (2021). Copyright 2021 American Chemical Society.[30] (g) S11 reflection spectra of SAW devices with varying Al plate thicknesses with their

typical peaks in the spectra identified through FEA simulations. Reproduced with permission from Tao et al., Sci. Rep. 8(1), 1-9 (2018). Copyright 2018 Spring Nature.[98]

3.3 Bending Behaviors of Flexible SAW Devices

Deformation behavior of piezoelectric thin film/flexible substrate SAW devices under working conditions is often strongly dependent on the flexible substrate.[99] For example, thinned silicon chips, polymers, and flexible glass are mainly subject to elastic deformation,[20,33,34,40] whereas metal foils generally show non-uniform elastoplastic deformation behaviors. These deformations will cause changes in characteristics of acoustic wave propagation, especially for acoustic velocity and resonant frequency, which will be discussed in detail in this section.

3.3.1 Elastic Deformation for Layered Flexible SAWs

For the elastic bending deformation of layered flexible SAW devices, a general bending behavior model is schematically illustrated in **Figure. 4a,** in which θ is the bending angle and α refers to the off-axis angle between the direction of SAW propagation and direction of bending strain. Acoustic wave velocities as functions of external stresses or bending strains can be described by considering the varied applied strains.[100] Therefore, the coupling wave equations of an acoustic wave device can be written as.[90]

$$\sigma_{jk}\frac{\partial^2 u_i}{\partial x_j \partial x_k} + C_{ijkl}\frac{\partial^2 u_k}{\partial x_l \partial x_j} + e_{jkl}\frac{\partial^2 \phi}{\partial x_k \partial x_j} = \rho\frac{\partial^2 u_i}{\partial t^2} \tag{1}$$

$$e_{jkl}\frac{\partial^2 u_k}{\partial x_l \partial x_j} - \varepsilon_{jk}\frac{\partial^2 \phi}{\partial x_k \partial x_j} = 0 \tag{2}$$

where σ_{jk} is the initial stress; ϕ is the electrical potential; ρ is the density; u is the mechanical displacement, e_{jkl}, C_{ijkl},and ε_{jk} are piezoelectric constants, elastic stiffness constants, and dielectric constants, and $i, j, k, l = 1, 2, 3$. Solutions of Eqs. (1) and (2) can be obtained using the following traveling-wave equation.[100]

$$u_k = \mathrm{e}^{\mathrm{j}\omega t}\beta_k \exp\left[-\mathrm{j}\frac{w}{v}(x_1 + \gamma x_3)\right] \ (k = 1,2,3) \tag{3}$$

$$\phi = \mathrm{e}^{\mathrm{j}\omega t}\beta_4 \exp\left[-\mathrm{j}\frac{w}{v}(x_1 + \gamma x_3)\right] \tag{4}$$

where w is the steady-state angular frequency, v is SAW velocity, and γ is the exponential decay constant in direction x_3, . By substituting Eq. (3) and (4) into Eqs. (1) and (2), we can obtain a similar form of Christoffel equation.[89] For a layered SAW device, these boundary conditions for both the piezoelectric layer and substrate can be found from the Ref.[101] Under the restriction of boundary conditions, acoustic velocity can be determined by a method of iteration.

Under the applied stress, three independent factors could change the wave velocities, i.e., initial stress (σ_{jk}), material elastic constants (C_{ijkl}), and material density (ρ).[90]Acoustic velocity at different off-axis angles and strains can be obtained using the new parameters to replace the original parameters.

The frequency shift (Δf) of the flexible acoustic wave devices under a bending condition can be calculated by combining the acoustic velocities changes and IDT deformation, i.e., the relative change of wavelength ($\Delta\lambda/\lambda$).

$$\Delta f = (\Delta v/v - \Delta\lambda/\lambda) \cdot f_0 \quad (5)$$

where f_0 is the frequency without appliedstrain.

In 2020, Ji et al. fabricated AlN/flexible glass based SAW and used the above model with a MATLAB program to study device's bending performance at various strains (0-1000 με) and off-axis deformation (0~90°). They found that the frequency shifts of the SAW device are highly dependent upon wavlength, bending strain and off-axis angle. With the increase of wavelength, results showed that the strain sensitivity is decreased significantly because of the decreased resonant frequency. In addition, a good linearity was observed for the frequency-strain responses at different off-axis angles, and the sensitivity became decreased with the off-axis angle α.[33] Furthermore, they also discussed the respective contributions of all the factors (including IDT dimensions, material elastic constants, initial stress, and material density) to the frequency shifts under different strains, and pointed out that the main contribution factor to the strain frequency shift of AlN/flexible glass SAW device is the initial stress as show in **Figures 4b&c.**[33]

3.3.2 Non-uniform Elasto-plastic Deformation for Layered Flexible SAWs

When using flexile substrates such as metal foils, the strain change or deformation is not a linear process. For non-uniform elastic-plastic bending, the stress-strain relationship of deformation caused by the external stress is different from that of uniform elastic bending, as shown in **Figure 4d** (using the Al foil as an example).[102] In order to obtain the resonant frequency of the elasto-plastic deformation region, two extreme conditions (corresponding to upper and lower boundaries of the resonant) are considered. The first condition is that the external stress is not released (at point 'C' shown in **Figure 4d**) and the tangent modulus is defined as k_c as shown in **Figure 4e**. The second condition is that the external stress is fully released (at point 'D' in **Figure 4d**) and the tangent modulus is described using the empirical formula as shown in **Figure 4e**. Based on the above analysis and multisublayer stiffness matrix method,[103] Zhang et al. solved the theoretical resonant frequency of the flexible SAW device with ZnO/Al foil layered structure under a bending state using a MATLAB program.[102] For this

bilayer structure, its coordinate system can be obtained as shown in **Figure 4f, and** its strain distributions are shown in **Figure 4g**. The corresponding frequency shifts are shown in **Figures 4h&i**. **Figure 4j** shows the combined frequency shift of the SAW device. From these results, we can observe that the elastic region becomes much "narrower" and the elasto-plastic region becomes much "wider" under the strain.[102] Furthermore, based on the experiment of bending ZnO/Al flexible SAW devices, condition 1 can be used for accurate calculation of elastic region, and condition 2 can be used to predict the general trend of large elastic plastic region, as shown in **Figure 4j**.[102]

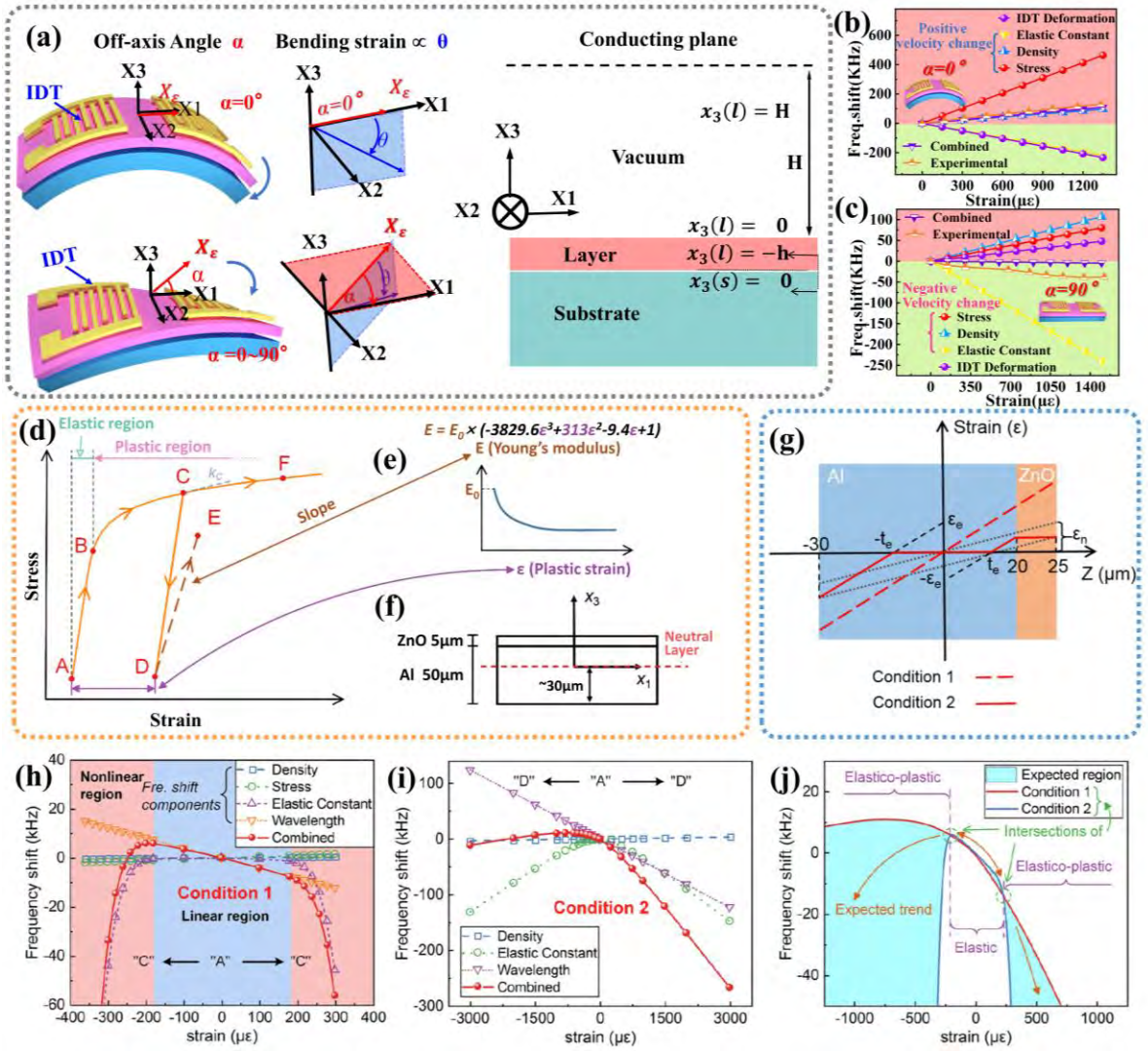

Figure 4 (a) Illustrations of flexible and layered SAW devices at various off-axis angles and bending strains; Comparison of experimental frequency shifts and theoretical frequency-strain responses for AlN/flexible glass SAW device at off-axis angles of 0° (b) and 90° (c), with λ = 20 μm. Reproduced with permission from Ji et al., Microsyst. Nanoeng. 7, 97 (2021). Copyright 2021 Springer Nature.[33] (d) Stress-strain curve for ZnO/Al device during loading (path "ABCF"), unloading (path "CD") and reloading (path "DE"); (e) Relationship between Young's modulus and plastic strain after unloading represented by point "D"; (f) Coordinate system and neutral layer used to calculate strain/stress distributions for the flexible ZnO/Al SAW

devices during pure bending. (g) Strain distribution in the ZnO/Al flexible SAW devices under conditions 1 and 2 with nominal stress exceeding the elastic limit of Al substrate. Total frequency shifts calculated from changes of density, stress, elastic constant, and wavelength as a function of strain in condition 1 (h) and with funcitons of density, elastic constant, and wavelength in condition 2 (i). The expected frequency shift region and trend determined by these two extreme conditions (1 and 2) is shown in (j). Reproduced with permission from Zhang et al., Appl. Phys. Lett. 118, 121601 (2021). Copyright 2021 American Institute of Physics.[102]

4. Flexible Acoustic Wave Sensors

SAW sensors are sensitive to the changes of acoustic wave propagation parameters such as phase velocities of an acoustic wave device due to the various physical parameters.[104-106] Equation (6) elucidates changes of wave velocities due to changes in mechanical, electrical, mass, and environmental properties. Here v is the wave velocity in substrate, and it is functions of multiple physical/chemical parameters, including mass (m, generally called mass loading effect, e.g., particles, humidity, gas or biomolecules), electrical properties (e.g., conductivity, often called electrical loading effect), mechanical properties (M_i, e.g., elastic modulus or viscosity, sometimes called elastic loading effect), and environment factors (e_v, which include temperature, or can called environmental effects). The following equation can be used to describe all these influences.[36]

$$dV = (\frac{\partial V}{\partial m} dm + \frac{\partial V}{\partial E} dE + \frac{\partial V}{\partial M_i} dM_i + \frac{\partial V}{\partial e_v} de_v) \quad (6)$$

All these influences will lead to changes of acoustic wave velocity, thus shift the resonant frequency. By detecting the resonant frequency shift, we can extract changes of physical or chemical or environmental parameters, thus the SAWs can be effectively used as sensors. These have been well-documented in many review papers for SAW sensors.[35,107-111]

Flexible SAW sensor can be applied on the curved surface, which broadens the application range of SAW sensors. Some studies proved that flexible SAW has great application potential as an electronic skin,[26] and it is true that the biggest application area of flexible SAW is the sensors used in body or in curved scenes. In the following sections, SAW applications for flexible temperature sensors, strain sensors, humidity sensors, ultraviolet sensors, chemical sensors, biosensors, and acoustofluidics lab-on-a-chip system are discussed.

4.1 Flexible Acoustic Wave Temperature Sensor

It is very important to use temperature sensors to monitor physiological activities, especially heat transfer between biological tissues and the environment. SAW temperature

sensor measures the external temperature changes through monitoring the changes of SAW resonant frequency due to variations of the SAW velocity and changes of interdigital electrode distance.[112,113] Because of its small size, light weight and wireless passive advantages, the conventional SAW devices can be used to monitor temperature changes in high-temperature furnace, heating plant, process room, motor shaft and vehicle brake. However, due to their key issues such as stiff, rigidity, brittleness and biological incompatibility, these conventional rigid SAW devices are difficult to conformally apply onto various shapes of the structures or human skin. Flexible SAW devices can be used to continuously monitor the local temperature changes on the skins, monitor or agitate the biological tissues, understand the thermal causes of intra-body balance, and detect various health conditions.

High sensitivity is crucial for these flexible SAW temperature sensors. Therefore, previously various researchers tried to increase the TCF value of flexible SAW temperature sensors by using substrate materials with large expansion coefficients and optimizing device structures. For example, Jin et al. prepared ZnO/PI based flexible SAW devices with a wavelength of 20 μm **(Figure 5a)**, and the resonant frequencies were decreased linearly with temperature (**Figure 5b**). Accordingly, TCF values of 442 and 245 ppm/°C were obtained for the Rayleigh and Lamb modes, respectively.[29] Tao et al. reported the changes of TCF values as a function of normalized wavelength parameters (e.g., λ/h), as shown in **Figure 5c**. They changed the λ/h ratio and obtained a high TCF of −760 ppm/°C for ZnO/Al foil SAW device.[114] Lamanna et al. reported a flexible and transparent AlN-based SAW device on the PEN substrate, which shows a large TCF value of ∼810 ppm /°C for the Rayleigh wave. **Figure 5d** shows that a thermal camera image with the uniform heat conduction through AlN/PEN-based patch from the skin to the SAW devices, and **Figure 5e** shows that the obtained results from the SAW devices have a good linearity.[21]

None of the above studies have reported wireless passive functions or wearability. Because the polymer substrate has a significant sound loss, the thin film polymer substrate-based SAW device is not quite suitable for wireless interrogations. Instead, the substrate with its maximum sound transmission efficiency should be applied. In addition, it is also necessary to ensure that the sensor to obtain the consistent readings on a curved or bent surface. Some structures (e.g., net-shaped, island-bridge, paper-cut, serpentine ones) need to be applied and they can improve the skin conformability and stretchability.[115] Therefore, Floer et al combined a thinned and freestanding Z-cut $LiNbO_3$ substrate (with a thickness of 60 μm) and an antenna and fabricated a wireless and stretchable SAW temperature sensor (**Figure 5f**), which has a frequency of 858 MHz and a Q value of 4087. Its TCF value is-77 ppm/°C, and it also shows a good wireless sensing capability within an interrogation distance of 5 cm[86].

Although the research on flexible SAW temperature sensor has achieved some success, the following key problems are still unsolved.

- The stress and strain caused by the human body movement and the humidity generated by skin will interfere with the measurement results. On the contrary, this is also a dilemma for influences of other environmental parameters such as humidity, UV and strain. Although some methods have provided solutions for eliminating strain,[99] humidity and temperature,[116] these studies only show insignificant improvements.
- The resolution of the sensor is often a problem because the temperature change for the human body is very small.
- The substrate should always ensure a good conformability with the skin, and also have good thermal conductivity, wear resistance and comfort. For example, the thermal conductivity of polymer is very low, whereas the air permeability of Al foil is very poor.

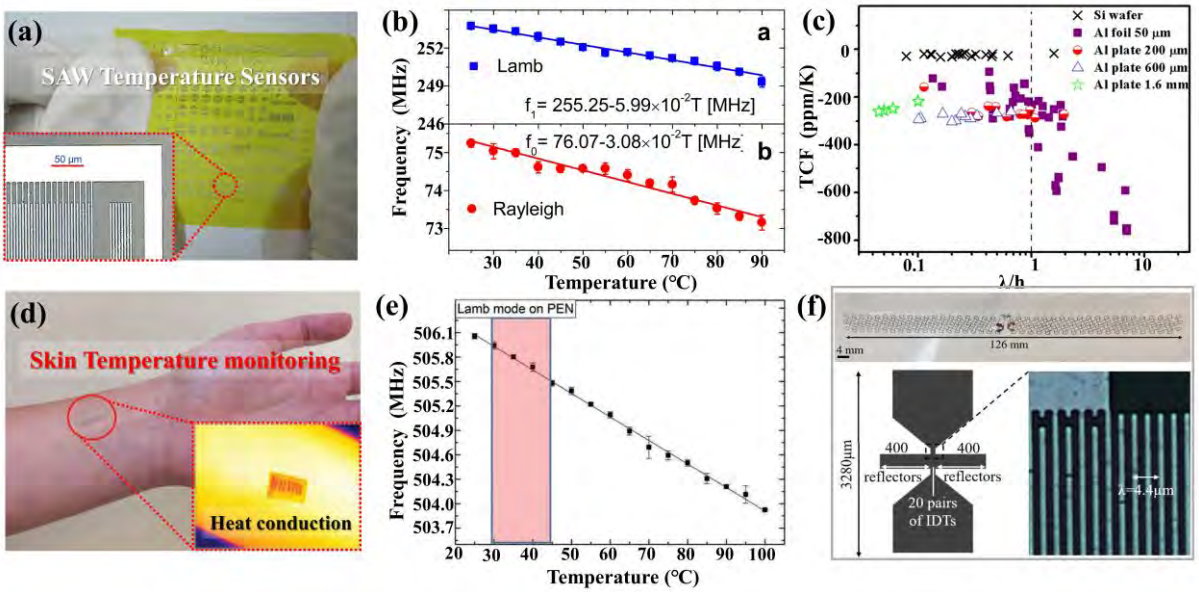

Figure5. Flexible SAW temperature sensor object display; (a) An image showing a SAW device with 20 pairs of IDTs; (b) The changes of resonant frequencies of the Lamb mode waves and Rayleigh mode waves varied with temperature. Reproduced with permission from Jin et al., Sci. Rep. 3, 2140 (2013). Copyright 2013 Springer Nature.[29] (c) A summary of TCF values of ZnO SAW samples on different Al substrates as a function of normalized wavelengths λ/h; Reproduced with permission from Tao et al., Sci. Rep. 8(1), 1-9 (2018). Copyright 2018 Spring Nature.[98] (d) Wearable SAW patch for temperature monitoring on skin; (e) An example of SAW frequency responses at varied temperatures; Reproduced with permission from Lamanna et al., Adv. Electron. Mater. 5(6), 1900095 (2019). Copyright 2019 Wiley-VCH Verlag.[21] (f) The design and structures of the wireless temperature SAW device with a photo of the testing device. Reproduced with permission from Flore et al., 2019 IEEE Sensors. 1-3 (2019). Copyright 2019 Institute of Electrical and Electronics Engineers Inc.[86]

4.2 Flexible Acoustic Wave Strain Sensor

The SAW strain sensors are based on frequency changes due to the velocity changes of SAW devices and the changes of distance for IDTs under the applied stress or strain. In the past a few years, SAW strain sensors based on the conventional rigid SAW devices have been proposed for automobile, aerospace, nuclear power and power generation industries.[117-120] However, due to the rigidity of these bulk devices, the strain sensing ranges of all these SAW sensors are limited to less than 400 με[121]. Flexible SAW strain sensors have attracted much attention due to their good flexibility, and they can be integrated into electronic devices or attached to curved surfaces and human skins. They can not only detect physical movement and health status of muscle/skin and pulses, respiration, vocalization and heartbeat, but also detect large strains such as body movements or bending of robot joints.

To meet the detectivity requirements, tremendous efforts have been made to improve the sensitivity and the strain range by changing flexible substrate materials and improving deposition quality of piezoelectric films. For example, He et al. fabricated ZnO/PET flexible SAW devices as shown in **Figure 6a**. The maximum measured strain was ~3500 με, and the sensor was still working under 100 cycles with a large strain of 2500 με[34]. However, it is not suitable for measuring large strains, because the deposited ZnO film on polymer has poor adhesion and is prone to cracking and peeling-off under repeated bending processes. In addition, the mechanical strength and wear resistance of polymers are poor, which limits the sensitivity and strain range of these flexible SAW strain sensors.

To solve the above problems, ultra-thin glass and piezoelectric single crystals are adopted for making these strain sensors. For example, Chen et al. deposited high-quality ZnO thin films on the ultra-thin flexible glass (i.e., Corning® Willow® Glass) and prepared flexible transparent SAW devices as shown in **Figures 6b**. Compared with the SAW devices on a rigid glass substrate, these flexible devices maintained good transmission characteristics, and provided good flexibility. The measured strain was d ± 3000 με[40], and the sensitivity of the device was ~138.9 Hz/με at the optimal annealing temperature of 200 °C.[20]

For flexible glass-based SAW device, the quality of piezoelectric films directly affects the detection range, repeatability, fatigue strength, and sensitivity of the SAW sensors. In 2018, Xu et al. fabricated flexible single crystal $LiNbO_3$ film-based SAW sensor with its thickness of 58 μm as shown in **Figure 6c**, and device showed double resonance modes (Raleigh and thickness shear mode). The measurement strain range could reach up to ±3500 με, and the sensitivity was 193 Hz/με. Its maximum hysteresis was less than 1.5%, and no obvious deterioration was found after hundreds of cycles.[38]

In 2021, Feng et al. fabricated SAW flexible strain sensors on an AT-X quartz plate with a thickness of 31 μm, as shown in **Figure 6d.** Its maximum measurement range is 5000 με with an excellent linearity, and the sensitivity was high up to 251.9 Hz/με. In addition, due to quartz is insensitive to temperature, the obtained SAW device showed a very low frequency temperature coefficient.[18] Li et al. reduced the thickness of a piezoelectric layer of (72%)Pb(Mg1/3Nb2/3)O_3-(28%)$PbTiO_3$ (PMN-PT) from 500 μm down to 37 μm using a chemical mechanical polishing method, and the sensitivity of such a SAW strain sensor was increased up to ~1243.49 Hz/με.[19]

Recently, Ji et al.[33] found that if the bending direction of the flexible SAW is different from the acoustic wave propagation direction (which means that there exists an off-axis deformations between the acoustic-wave propagation direction and bending direction), the strain sensitivity will be totally different. This indicates that the strain sensitivity could be adjustable by setting the various off-axis deformations. They prepared SAW devices with high-quality AlN thin films on flexible glass substrates, and demonstrated that[90] with the increase of off-axis angle α from 0 to 75°, a good linearity of frequency-strain was still maintained for the flexible acoustic wave devices at different off-axis angles. The frequency-strain sensitivity was also observed to decrease when the off-axis angle α was increased (**Figure 6e**). The flexible SAW human motion detection was also conducted to verify this adjustable strain sensitivity with various off-axis deformations (**Figure 6f).**

Table 3 summarizes development of flexible SAW strain sensing in recent years. Although these ultra-thin flexible SAW sensors have shown the significantly improved performance (e.g., sensitivity and measurement range), there is always an issue of incompatibility between the ultra-thin glass/single crystal and human skin. The sensor with good flexibility could have problem to attach strongly onto the skin with a hierarchically textured surface, or under complex natural motions. Kim et al. fabricated wireless e-skin structures using acoustic wave sensors based on ultrathin single-crystalline GaN membranes. They integrated ultra-thin and lightweight functional layers (GaN and metal electrodes) onto the polydimethylsiloxane (PDMS; ~20 μm). These GaN SAW devices showed good skin conformability, long-term wear resistance, and can reach 10.3% tensile strain, as shown in **Figure 6g**. They also demonstrated the wireless measurement of carotid artery and pulse (**Figures 6h&i**).

For flexible SAW strain sensors, there are still many issues which need to be investigated:

- Developing SAW devices with a larger strain range is crucially needed. The measured range of traditional metal foil-based strain gauge can reach 50000 με, but many of these flexible SAW strain sensors only reported 10% of that value.
- The existing flexible SAW strain sensors can only achieve simple bending deformation,

but cannot achieve a complex deformation (e.g., twisting, stretching, or tearing), and they are often fragile and brittle.

- The fatigue resistance is required for cyclic actuations in various applications. Many flexible sensors (other type) showed very good stability after 10,000 cycles at expansion/ compression in durability tests, but the developed flexible SAW strain sensor can only be curved with durability less than 1000 cycles.

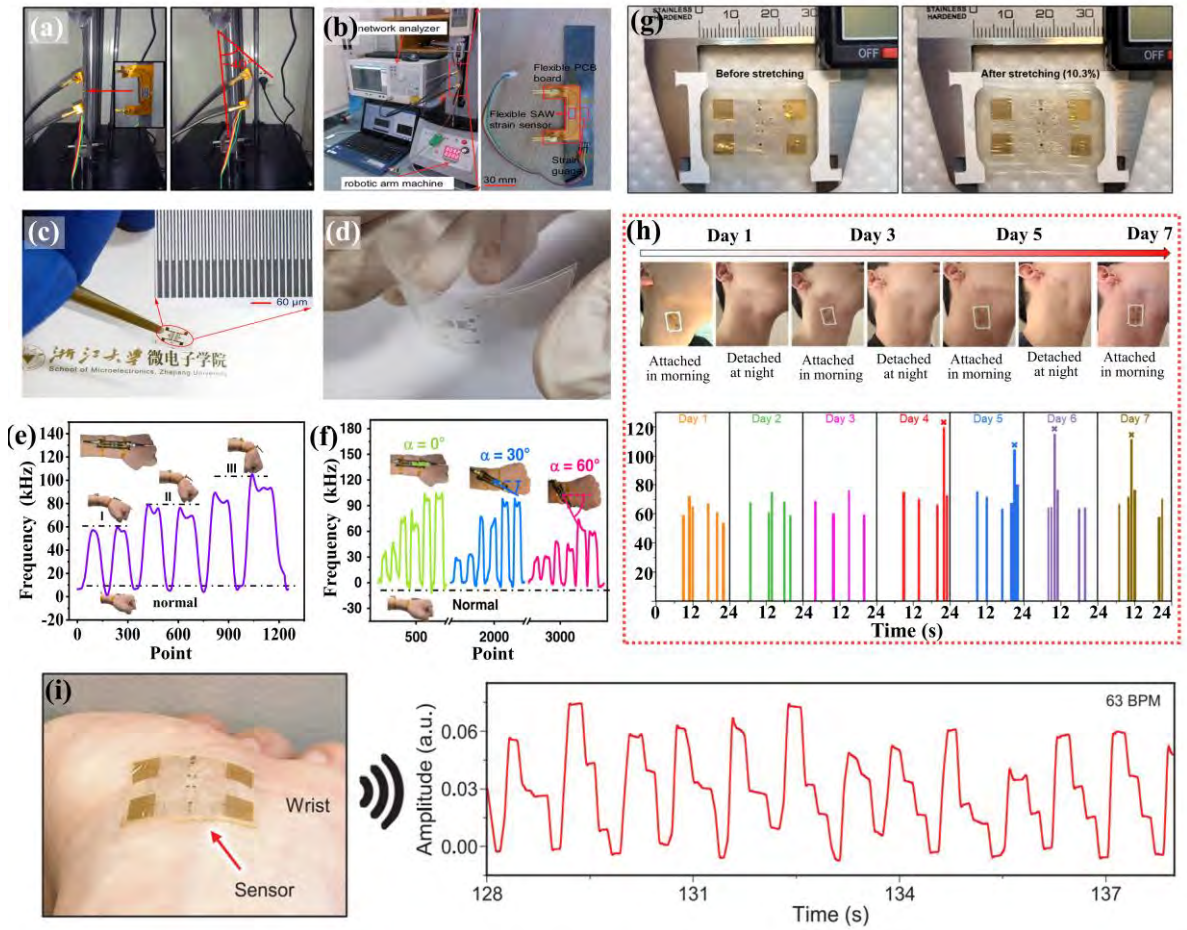

Figure.6 Flexible strain sensor performance chart. (a) An image shows a ZnO/PET SAW device before and after a 40-degree bend; PET Substrate; Reproduced with permission from He et al., Appl. Phys. Lett. 104, 213504 (2014). Copyright 2014 American Institute of Physics.[34] (b) An image displays the experimental setup for the bending test and a close-up photograph of the sensor. Reproduced with permission from Chen et al., J. Mater. Chem. C, 2, 9109-9114 (2014). Copyright 2014 Royal Society of Chemistry.[40] (c) a photograph of the SAW devices on flexible $LiNbO_3$. Reproduced with permission from Xu et al., J. Micromech. Microeng. 29, 025003 (2019). Copyright 2019 IOP Publishing Ltd. (d) a photograph of the SAW devices on flexible Quartz. Reproduced with permission from Feng et al., IEEE Sens. J. 21(17), 18571-18577 (2021). Copyright 2021 Institute of Electrical and Electronics Engineers Inc.[18] (e) Frequency shifts of the flexible SAW devices at different wrist bending states and (f) at off-

axis angles α of 0, 30, and 60°; Reproduced with permission from Ji et al., Microsyst. Nanoeng. 7, 97 (2021). Copyright 2021 Springer Nature.[33] (g) Photographs of GaN SAW-based e-skin before and after stretching (strain = 10.3 %). (h) Assessment of GaN SAW-based e-skin's reusability and long-term wearability. (i) Wireless pulse measurement using GaN SAW strain sensors in e-skin form. Reproduced with permission from Kim et al., Science, 377(6608), 859-864 (2022). Copyright 2022 American Association for the Advancement of Science.[26]

Table 3. Recent development and characteristics of flexible SAW strain sensors

Device structure	Frequency (MHz)	Strain range(με)	Sensitivity (Hz/με)	Cycle index	Hysteresis	TCF (ppm/°C)	Ref.
ZnO/PEN	110.7	2500	130	100	None	None	34
ZnO/glass	133.2	±3000	34.7	10	None	None	20
ZnO/glass	137.1	2000	138.9	1000	None	None	40
$LiNbO_3$ film	325	±3500	193	> 100	1.5%	-85	38
PMN-PT film	129	1000	1243	None	None	None	19
PEN/AlN	190(R) 500(L)	429 181	577 1156	None	None	None	122
Quartz AT-X	156.16 260.15	5000	186.2 251.9	None	None	-1.06	18
AlN/glass	290.13	1323	180.08 (adjustable)	1000		None	33

4.3 Flexible Acoustic Wave Humidity Sensor

As one of important environmental parameters, humidity is closely related to industry, agriculture and human life. Therefore, humidity sensors play an important role in environmental monitoring.[123,124] The working principle of SAW humidity sensor is mainly based on mass loading effect, and of course electric loading are also contributed. So far, real-time and non-contact monitoring of the concentration of water molecules released by the human body has been a challenge for humidity monitoring, which is directly related to vital signs, namely, respiratory arrest and respiratory frequency. Flexible SAW humidity sensor could be developed as one of the most potential methods for such a real-time monitoring of human humidity levels.

The flexible SAW humidity sensor is generally composed of a flexible SAW device with a top sensing layer for enhancing the humidity sensing. The common fabrication methods for this sensing layer include drop coating, spin coating and spray coating. Drop-coating has not required for any special humidity-sensing materials and is easy for operation. Spin-coating can

achieve precisely controlled and uniform thickness of the humidity sensing film. Another common method is spraying coating. It includes a high-pressure gas pipe and a spray gun.

Up to now, various humidity-sensing materials have been reported for SAW humidity sensors, including ZnO thin films, ZnO nanostructures (e.g., nanowires, nanorods and nanobelt), and two-dimensional materials such as graphene, oxides, and their composites. ZnO is a hydrophilic material and water molecules can be easily absorbed on its surface in a humidity environment. For example, He et al. prepared a flexible SAW-based ZnO/PI humidity sensor, and sensitivity of 3.5 KHz/%RH was obtained. Without any surface treatment, it already showed a good repeatability from the humidity of 5%–87%RH cycle.[62] Xuan et al. demonstrated a ZnO/PI humidity SAW sensor with a temperature compensation function (**Figure 7a**). The sensor shows two resonant frequencies with different TCFs, and one of these two frequencies is applied for temperature compensation, thus minimizing the temperature Influences.[21]

Compared with dense ZnO thin films, ZnO nanostructures have numerous loosely and porously interconnected 3D network structures with large specific surfaces and porosities. Tao et al. spin-coated ZnO micro-structure and nano-structure network (T-ZnO MN) as sensitive layers onto ZnO/Al foil SAW devices, as shown in **Figure 7b.** Under 90 %RH, the humidity sensitivity was increased by 2.9 times compared with that without using T-ZnO MN flexible SAW device (**Figure 7c**). It is noteworthy that after using T-ZnO MN, the sensing performance of respiratory characteristics was increased by ~1.7 times under the bending conditions.[125]

Carbon based materials (e.g., graphene, graphene oxide or GO, and graphene quantum dots) have also been widely used in humidity sensors because they can increase the active adsorption sites. For example, Wu et al. developed an ultra-thin glass based flexible and transparent SAW humidity sensor (**Figures 7d**) using graphene quantum dots modified ZnO nanowires as the sensitive film. The sensitivity of the device is as high as 40.16 KHz/%RH. **Figures 7e&f** show that human respiratory humidity can be detected. The flexible SAW sensor was attached to a curved surface. The device was bent with a bending angle of 30°, and its performance has not shown any apparent degradation (**Figure 7g**).[22]

Moreover, with the inherent wireless and passive monitoring functions, the humidity sensors can be applied onto the human body or embedded in clothes for obtaining sensing signals of physiological information from body movements. For example, Jin et al. reported a wireless passive ZnO/PI flexible SAW respiratory monitoring device to detect obstructive respiratory syndrome, as shown in **Figures 7h.** The breathing air with its changing humidity level can be detected by measuring the offsets of the resonant frequency of the SAW sensor. Therefore, any phenomena of obstructive sleep apnea of patients can be detected in real time.

An integrated planar antenna was also added to the sensor, while the electronics of other transmitters and receivers were separative positioned. They have demonstrated a wireless communication range of several meters for a duration of several hours, which can provide sufficient mobile space for the patient[23].

At present, many researchers are committed to improve sensitivity using the high-performance sensitive materials or to increase the device's frequency. However, there are many problems existed. For examples, the properties of the sensitive film will change under the device deformation conditions, or the repeatability of the preparation of the sensitive film is poor.

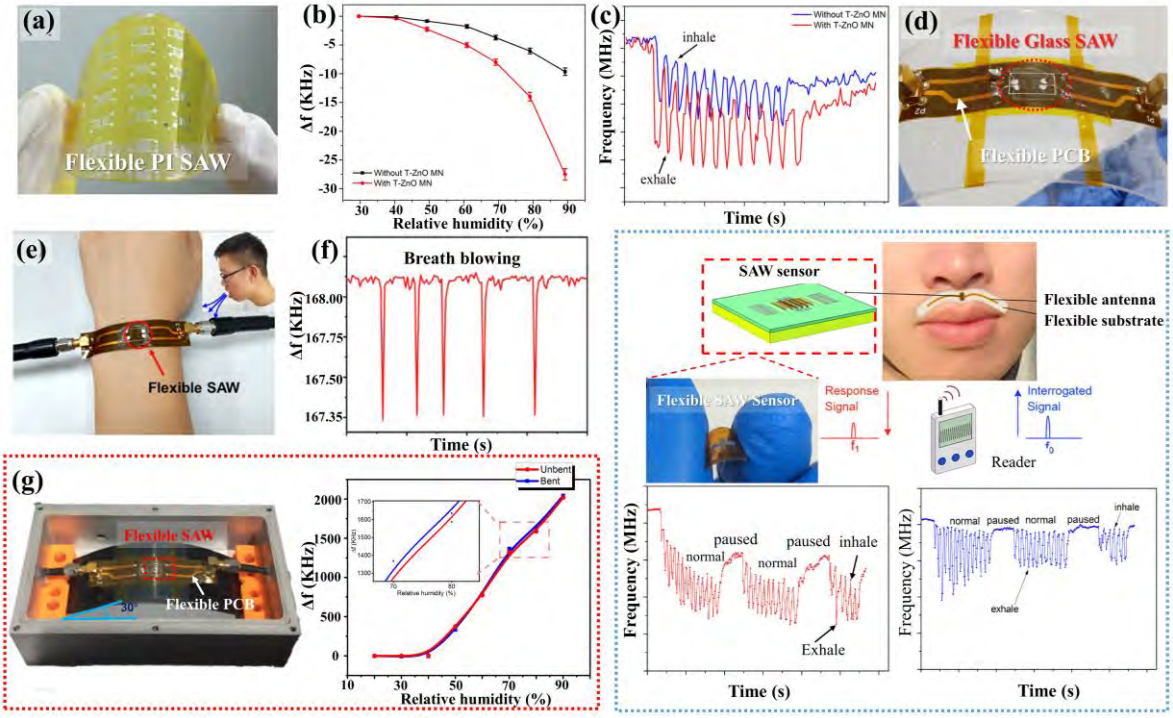

Figure7. (a) Image of a flexible SAW device on PI substrate; Reproduced with permission from Xuan et al., Procedia Engineering, 120, 364-367 (2015). Copyright 2015 Elsevier Ltd.[24] (b) Comparisons of humidity responses for flexible SAW sensors without/with T-ZnO MNs; (c) Resonant frequency changes for flexible SAW sensors with and without T-ZnO MNs during uniform and continuous respiration; Reproduced with permission from Tao et al., ACS Appl. Nano Mater. 3(2), 1468-1478 (2020). Copyright 2020 American Chemical Society.[125] (d) Flexible SAW device packaged with polyimide PCB and mounted on PET; (e) Experimental setup for breathing detection using flexible SAW attached on the wrist; (f) Frequency changes in flexible SAW humidity sensor after 5 breathing cycles, with SAW device wavelength of 16 μm. (g) Photograph of flexible SAW sensor in a bent state, and frequency shifts of flexible humidity sensor (λ=12 μm) in both unbent and bent conditions, with a bend angle of 30°; Reproduced with permission from Wu et al., ACS Appl. Mater. Interfaces, 12, 39817-39825 (2020). Copyright 2020 American Chemical Society.[22] (h) Schematic illustration of sensing

mechanisms and measurement data of the proposed wireless, passive SAW respiration sensor system. Reproduced with permission from Jin et al., J. Micromech. Microeng., 27, 115006 (2017). Copyright 2017 IOP Publishing Ltd.[23]

4.4 Flexible Acoustic Wave UV Sensor

UV light is applied for biomedical applications, space communication, astronomy, and water treatment. The sunlight containing ultraviolet rays is beneficial to the human body because it can synthesize vitamin D, but it can cause skin cancer and other types of skin diseases when the skin is exposed to excessive sunlight.[126] Therefore, it is critical to monitor the UV dosage and exposure levels.[127] The UV detector based on flexible SAW technology has the unique advantages with wearable and wireless operation capabilities. The key principle for UV sensing is that upon irradiation of UV light, there is an apparent shift in resonant frequency of the flexible SAW sensor, which can be attributed to acoustoelectric effects caused by surface adsorbed oxygen species and thermal effects caused by the UV source.[116] UV sensing material is the key component of flexible SAW UV sensor, which directly determines the sensitivity, response/recovery time, linearity and repeatability of the sensor. The most commonly used UV sensitive materials are ZnO and its micro- and nanostructures, because of its outstanding properties, ease of preparation and its bandgap width of 3.4 eV.[127,128,129] For example, He et al. prepared a dual-mode (i.e., Rayleigh and Lamb modes) flexible ZnO / PI SAW UV sensor and studied its UV sensing performance, with some results shown in **Figure 8a**. The UV sensitivities of those two modes are 111.3 and 55.8 ppm$(mWcm^{-2})^{-1}$, respectively(**Figure 8b**).[44]

ZnO nano- and microstructures have unique mesoscopic physical properties such as large specific surface area and quantum confinement, and thus they have excellent properties for UV detection. For example, Yin et al. used graphene quantum dots modified zinc oxide nanowires to enhance the UV sensing performance of ZnO SAW devices on an ultra-thin glass (**Figure. 8c**). As shown in **Figure 8d** , the results showed that the sensitivity was increased by three times compared with the device without using such a sensing material, and the flexible sensor was also maintained good performance at 30° (**Figure 8e**) bending angle for 200 times without obvious degradation.[25] Hasan et al. fabricated ZnO/Al foil SAW sensor with hydrothermally processed ZnO nanorods as the sensing layer. The SAW UV sensor has good sensitivity and reliability at different bending positions including flat, bending up and down. A nearly linear relationship of frequency shift was observed with UV intensity and the respond time was as small as ~10 s. The sensitivity values of the sensor were 56.2 ppm$(mW/cm^2)^{-1}$ and 27 ppm$(mW/cm^2)^{-1}$ for both A0 and S0 modes of the Lamb waves (**Figure 8f**), respectively.[127]

Kim et al. reported the chip-less and wireless e-skin based GaN SAW sensor which is

sensitive to the UV light. **Figure 8g** shows that the wireless GaN SAW UV sensor received UV light through polyimide through-holes, and conductivity of GaN film was changed and the responses of UV sensors were changed accordingly. **Figure 8h** shows the results of response and recovery speeds and also the selectivity for UV light compared to the white light for single-crystalline and multi-crystalline GaN UV sensors.

Both SAW based UV and humidity sensors need sensitive materials to improve sensitivity, therefore, they face the same dilemma. Although it is generally considered that the principles of UV sensing include mass loading, acoustoelectric, and photo-capacitive effects, but no theoretical model can be perfectly used to explain experimental results of frequency shift of SAW devices under UV irradiations.[126] It has been reported that surface plasma can improve the light absorption of specific wavelength and the separation speed of electron hole pairs.[130]

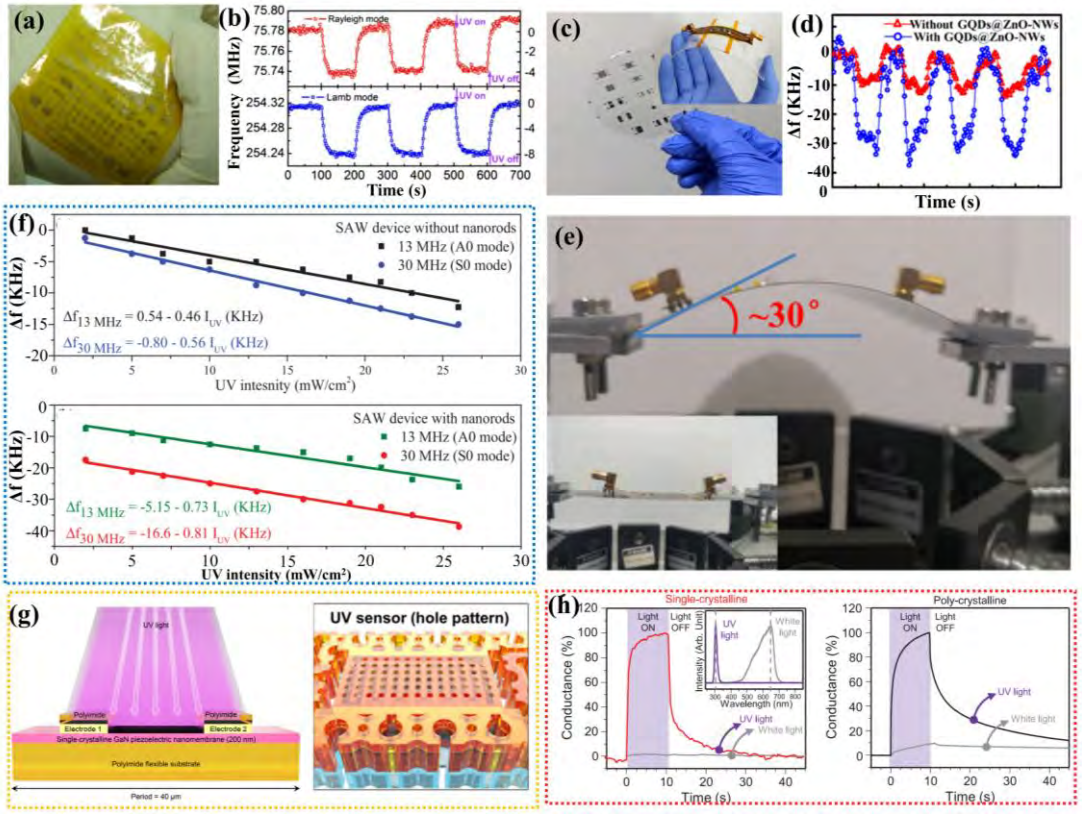

Figure 8. (a) Image of the flexible UV SAW sensors on a polyimide film; (b) Responses of resonant frequency of flexible SAW sensors to UV light illuminations for a few cycles; Reproduced with permission from He et al., J. Micromech. Microeng., 24, 050014 (2014). Copyright 2014 IOP Publishing Ltd.[44] (c) Flexible SAW devices on 3-inch glass wafer, diced and packaged onto flexible PCB; (d) Repeatability testing results of devices with and without a GQDs@ZnO-NWs sensitive layer under a light intensity of 50 mW/cm^2; (e) A maximum bending state of a flexible SAW polymer device; Reproduced with permission from Yin et al., Sensor Actuat. A-Phys. 15, 112590 (2021). Copyright 2021 Elsevier Ltd.[25] (f) Resonant frequency shifts for both zero order modes with and without nanorods under

varied UV intensities; (g) Wireless GaN SAW sensor for UV detection, including its structure and micrographs; (h) Response and recovery speeds for UV and white light in single- and polycrystalline GaN UV sensors. Reproduced with permission from Kim et al., Science, 377(6608), 859-864 (2022). Copyright 2022 American Association for the Advancement of Science.[26]

4.5 Flexible Acoustic Wave Chemical Sensor and Biosensors

In the past decades, great effort has been made to develop new biosensing technology for disease diagnosis, pollutant detection in water and food. With the development of robotics, internet of things (IoT) and medical sensors, new types of flexible sensor technologies are needed to produce low-cost, sustainable, reusable or recyclable materials. SAW based e-skin has recently been applied for wireless monitoring ion and sweat. **Figure 9a** schematically illustrates wireless e-skin measurement system, in which GaN film was made on PDMS patch using a transfer method to form acoustic wave devices onto PDMS patch such that the devices were aligned on top of the holes that penetrated through the patch. These acoustic wave devices were connected through patterned stretchable interconnects, which were linked to stretchable antenna. For achieving conformability, stretchability, and breathability, many dumbbell-shaped holes were patterned on these patches. The fabricated wireless ion sensors which are based on GaN SAW devices coated with Na+ ion–selective membranes are shown in **Figure 9b**. They were attached to the back of hands to record the concentrations of Na^+ in human sweat, and the concentration of Na^+ was gradually increased with the increase of skin temperature, as shown in **Figure 9c**.

Flexible devices based on SAWs have been used for pH, E. coli and glucose sensing. For instance, Tao et al. integrated thin film SAW technology with electromagnetic metamaterials, together using carbon fiber. The device can monitor environmental parameters and concentrations of biomolecules in a non-invasive, *in-situ*, and continuous manner through its wireless capability. Its sensitivity for detecting glucose concentrations is ~0.34 MHz/(mg/dL).[46] Lamanna et al. prepared a SAW immunosensor based on AlN coated PEN structures, which was applied to detect E. coli based on protein-A/antibody affinity (**Figure 9d**). This Lamb wave device showed a high sensitivity and high phase wave propagation on polymer substrate, and the mass of a single E. coli can be estimated using a finite element method.[27] Piro et al. developed a flexible AlN/PEN wearable PH SAW sensor (**Figure 9e**) with a central frequency of 500 MHz. They fabricated a SU-8 microfluidic channel with ZnO nanoparticles functionalized as a PH sensitive layer between IDTs, and the sensor showed a sensitivity of 30 KHz/PH from PH7 to PH2.[28]

Flexible SAW chemical sensors and biosensors have been developed extensively recently,

however, there are some key issues existed for their development.

- One of the key issues for the biosensor is to improve selectivity for a given recognition target, within an environment with the presence of multiple interfering elements.
- Further miniaturization and integration are needed to analyze smaller sample size and improve the sensitivity/selectivity of the flexible SAW biosensors.
- The biosensor should be low-cost, and requires much fewer sample volumes in-taken.
- Development of flexible, wearable, wireless, or self-powered and adaptable biosensors are needed.
- The flexible biosensors should be able to use by personnel with limited technical skill.

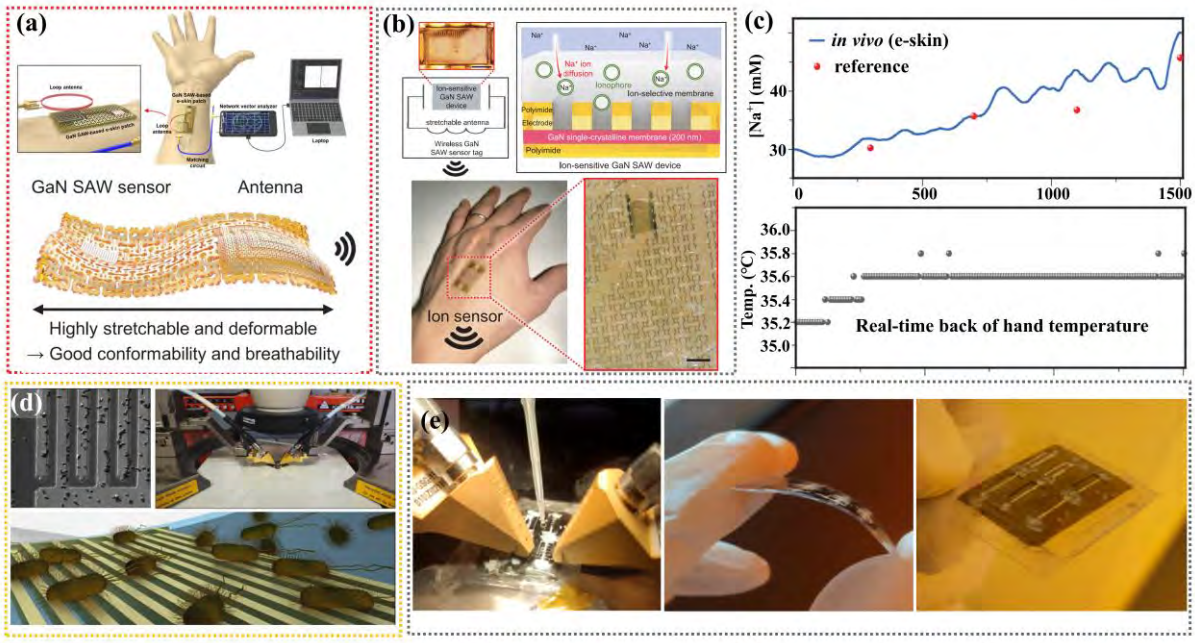

Figure.9 (a) Illustration of the wireless e-skin measurement system; (b) Resonant frequency shifts of GaN SAW ion sensor in responses to changes in Na+ ion concentration, (c) Recorded Na+ ion concentrations in sweat and skin temperatures from the e-skin measurement systems using wireless GaN SAW-based e-skin and a reference conductometer. Reproduced with permission from Kim et al., Science, 377(6608), 859-864 (2022). Copyright 2022 American Association for the Advancement of Science.[26] (d) IDTs, SAW device, testing and sensing illustration of flexible AlN-based SAW device used for sensing of *E. coli*. Reproduced with permission from Lamana et al., Biosens. Bioelectron. 163, 112164 (2020). Copyright 2020 Elsevier Ltd.[27] (e) Experimental images showing the SAW device's testing and electroacoustic measurements. Reproduced with permission from Piro et al., Nanomaterials, 11(6), 1479 (2021). Copyright 2021 Multidisciplinary Digital Publishing Institute.[28]

4.6 Flexible Acoustic Wave Sensors for Flow Control and Condensation

Flexible SAW devices have also been explored for sensing applications in other applications such as pipelines and agricultural environmental monitoring. In 2020, Zhang et al.

developed a flow rate measurement based on flexible ZnO/Al foil SAW devices (**Figure 10a**).[131] A heat source was incorporated to generate a temperature offset for the flexible SAW device, and the thermal equilibrium temperature of device provided the predicted values of gas flow rate. The flow rate was measured indirectly by the changes of the resonant frequency, which was influenced directly by the temperature of the device. Owing to the high coefficient of thermal expansion of the Al foil, a large TCF of ~280 ppm/K of the ZnO/Al foil SAW device could be obtained, resulting in an enhanced sensitivity and increased responses compared to other rigid SAW flow sensors (**Figures 10b-e**). In 2021, Zhang et al. presented a flexible smart patch which could detect and then eliminate the condensation on the structural surface (**Figure 10f**).[132] The flexible smart patch, composed of the flexible Lamb wave device and corresponding detection algorithm, detected the acoustic energy loss caused by condensation on the propagation path of the Lamb waves. It can subsequently eliminate the condensation through integrated dielectric heating and acoustic-thermal effect. Through a machine learning method, the responses to the vapor condensation could be distinguished from those due to temperature and humidity variations. The results of classification experiments showed a high precision of 94.40% (**Figure 10g**).

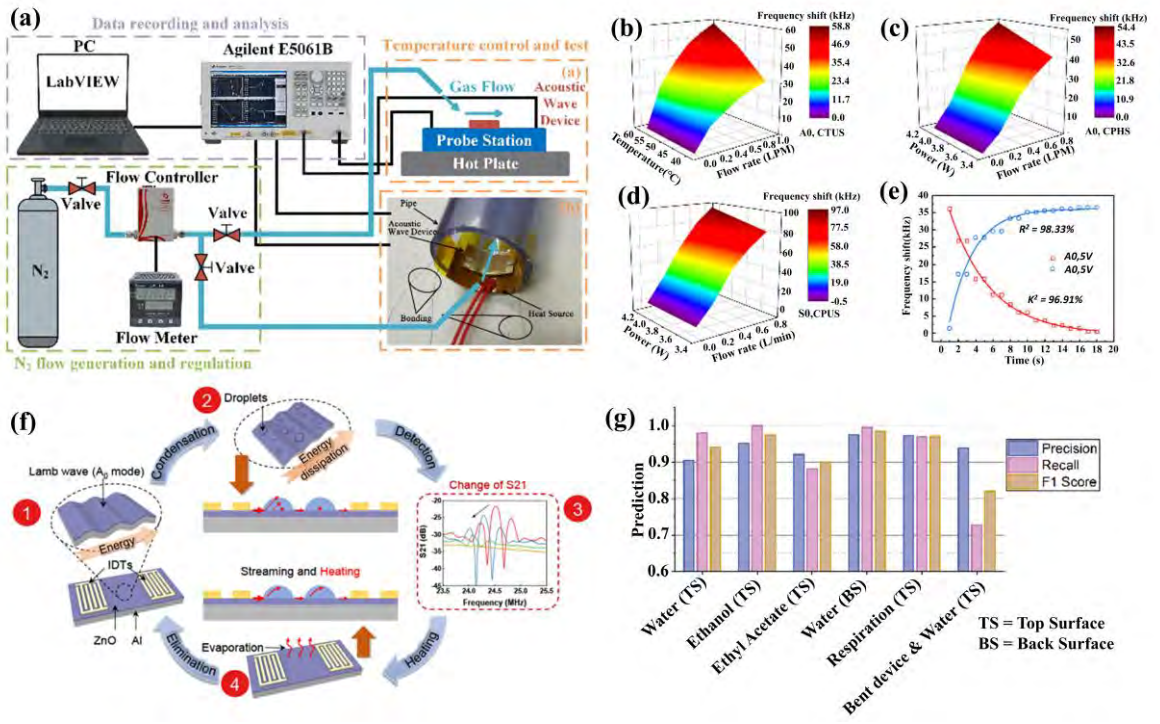

Figure.10. Flexible SAW devices for applications in flow rate measurement and condensation detection. (a) Experimental setup for flow rate, heating power/temperature, and resonant frequency shift measurement. 3D plots of frequency shifts for (b) A0, constant temperature heat source, (c) A0, constant power heat source, and (d) S0, constant power heat source. (e) Experimental data and fitted line plot of frequency shifts over time after changing flow rate from 0 to 0.8 litre-per-minute. Reproduced with permission from Zhang et al.,

J. Micromech. Microeng. 30, 095010 (2020). Copyright 2020 IOP Publishing Ltd.[131] (f) Schematic illustrations of condensation detection and elimination processes; (g) Classification results for distinguishing condensation and environmental interferences. Reproduced with permission from Zhang et al., ACS Sens. 6(8) 3072-3081 (2021). Copyright 2021 American Chemical Society.[132]

5. Flexible/Bendable Acoustofluidics and Lab-on-chip

Acoustic wave technologies are not only used for sensing but also used for acoustofluidics, which integrates acoustic wave technology and microfluidics. The commonly used acoustic waves for microfluidics include Rayleigh wave,[133-135] Lamb wave,[136] and bulk acoustic waves, as also including film bulk acoustic resonator (FBAR).[137,138] The mechanism of acoustic streaming is mainly due to acoustic velocity mismatch between the liquid and piezoelectric substrate, which changes the wave mode to a leaky mode and dissipating acoustic energy into the liquid medium to produce an acoustic streaming force to actuate the liquid droplet.[139] With proper surface texture/treatments and under enough applied power, the flowing liquid in a channel or a liquid droplet on the SAW propagating paths can experience streaming, vibration, pumping, jetting and even nebulization.[140,141]

For acoustic tweezer based acoustofluidics,[55] the force actuated on the particles are often called an acoustic radiation force, which can be applied to manipulate, pattern and sort those microparticles or biological cells. Within the liquid, the flow also induces streaming forces which can drive the flow of particles inside liquid. By utilizing of standing wave, slanted IDTs, or modifying alignment positions of microchannels, various functions or phenomena for particle counting, alignment, sorting and separation have been extensively reported.[11,142-144]

However, most conventionally made acoustofluidic devices are based on those bulk $LiNbO_3$ substrates,[145-148] or piezoelectric thin films (AlN and ZnO) on silicon, glass or Al plate.[149-153] Apparently, these substrates are rigid and fragile, thus are unsuitable for applications which strictly require functions including deformability and flexibility for being integrated into complex shapes and structures. It is a great advantage to be able to actuate liquids (either in droplet format or liquid in channels) along bendable, flexible, or randomly three-dimensional (3D) surfaces. This can easily realize wearable and 3D acoustic wave devices for wearable biosensors, drug delivery, and lab-on-a-chip diagnostics. Therefore, it is especially important to study flexible/bendable acoustofluidics for different industry applications.

To realize flexible acoustofluidics, the first step is the preparation of flexible devices. As mentioned above, there are generally two ways to fabricate flexible acoustic wave devices, either significantly reducing the thickness of conventional piezoelectric crystals, or depositing

piezoelectric thin films (with their thicknesses around several microns) onto the flexible non-piezoelectric substrates. The former often has issues of high synthesis costs and limited deformability due to the brittleness of the piezoelectric materials. Whereas the latter can provide fast and low-cost fabrication processes along with highly flexible nature of the substrate, which should have more potentials for acoustofluidic applications. It is worthwhile to point out that compromises are always needed to take between flexibility, power consumption efficiency and performance of these flexible acoustofluidics SAW devices.

For simplicity, acoustofluidics are usually divided into digital acoustofluidics and continuous acoustofluidics. The digital acoustofluidics are usually used to manipulate the liquid droplet on a chip, whereas the continuous acoustofluidics are often used to handle the liquid or particles in microchannels. There are many challenges for both of these flexible acoustofluidics applications:

- As addressed above, there is a severe compromise between device's flexibility and microfluidic performance. To obtain device's flexibility, it is required to significantly reduce the substrate thickness. However, it also reduces the device's stiffness, and thus results in device's easy deformation and acoustic energy dissipation into the flexible substrates after applied the RF power, thus degrading the acoustofluidic performance.
- There is a wave mode transition with the reduced substrate thickness. When the substrate thickness is larger than the device's wavelength, the acoustic wave mode is generally Rayleigh wave, with the reduce of substrate thickness to below one wavelength, the wave mode will change to hybrid mode or Lamb wave. It is commonly agreed that the microfluidic performance of Lamb wave is not as good as Rayleigh wave.
- It is needed to enable efficient liquid handing on curved surface. For microfluidic actuation on bended surface, on the one hand, it needs to provide a designated slipperiness for actuating the liquid droplet, on the other hand, it also requires enabling a sufficient stickiness for the retention of the liquid on the curved or inclined surface.
- A good bonding between the substrate of SAW device and microchannel is difficult to achieve. Even this can be solved before application, after the bending of the device, the microfluidic channel tends to break away from the substrate.
- There is a strong bending effect on particle manipulation. When the device is bended, the wave vibration mode may be changed, which have a significant influence on precise particle or biological species manipulations.
- The bending radius during deformation has a significant effect on bonding. When the bending radius of the device is smaller than several wavelengths, it is difficult to bond the channel onto the substrate in consideration of channel size.

In following sections, we will focus on recent development of flexible acoustic wave devices applied for both the digital acoustofluidics and continuous acoustofluidics.

5.1 Digital Acoustofluidics

Some commonly used polymers, including PI and PET, were firstly used as the flexible substrates for flexible acoustofluidics. However, there is severe acoustic wave dissipation into these "soft" substrates, thus resulting in an inferior microfluidic function. In 2013, Jin et al. for the first time reported a ZnO/PI based flexible acoustic wave device and achieved an acoustic streaming velocity of 3.4 cm/s with an applied voltage of 9.5 V (**Figure 11a**).[29] However, there was no any liquid transportation reported. In 2014, Wang et al. compared microfluidic performance of flexible ZnO/PI SAW device with those of conventional ZnO/Si and ZnO/glass SAW devices.[149] They showed that ZnO/PI SAW device present a poor microfluidic performance compared to those of ZnO/Si and ZnO/glass SAW devices, and only acoustic streaming and concentration were observed. The limited performance of SAW devices for acoustofluidics on polymer substrates is mainly due to wave energy loss through attenuation and dissipation within the substrate, as well as poor crystallinity and adhesion of thin films. Therefore, although the polymer substrates present a good flexibility, it is usually regarded as non-ideal for flexible acoustofluidics.

Metal, such as Al sheet/foils, have their advantages such as deformability and re-deformability, if compared with their polymer counterparts. These solutions address common problems in flexible SAW devices made from polymers, which are excessive energy dissipation and permanent deformation. In addition, these Al sheet or foil based substrates effectively promote growth of highly textured piezoelectric films such as ZnO, and show improved film adhesion and significantly reduced stresses.[154] In 2015, Liu et al. theoretically analyzed and experimentally demonstrated highly efficient, flexible and bendable acoustofluidics (including streaming and pumping functions) using ZnO/Al foil (with a substrate thickness of 50μm) SAW device[63] (**Figure 11b**). However, as the stiffness of Al foils is poor, the flexible Al foil-based SAW device often suffers from large self-deformation at a high applied power, which deteriorates the microfluidic performance when jetting or nebulization are required. Therefore, the substrate thickness needs to be optimized for achieving the best microfluidic performance.

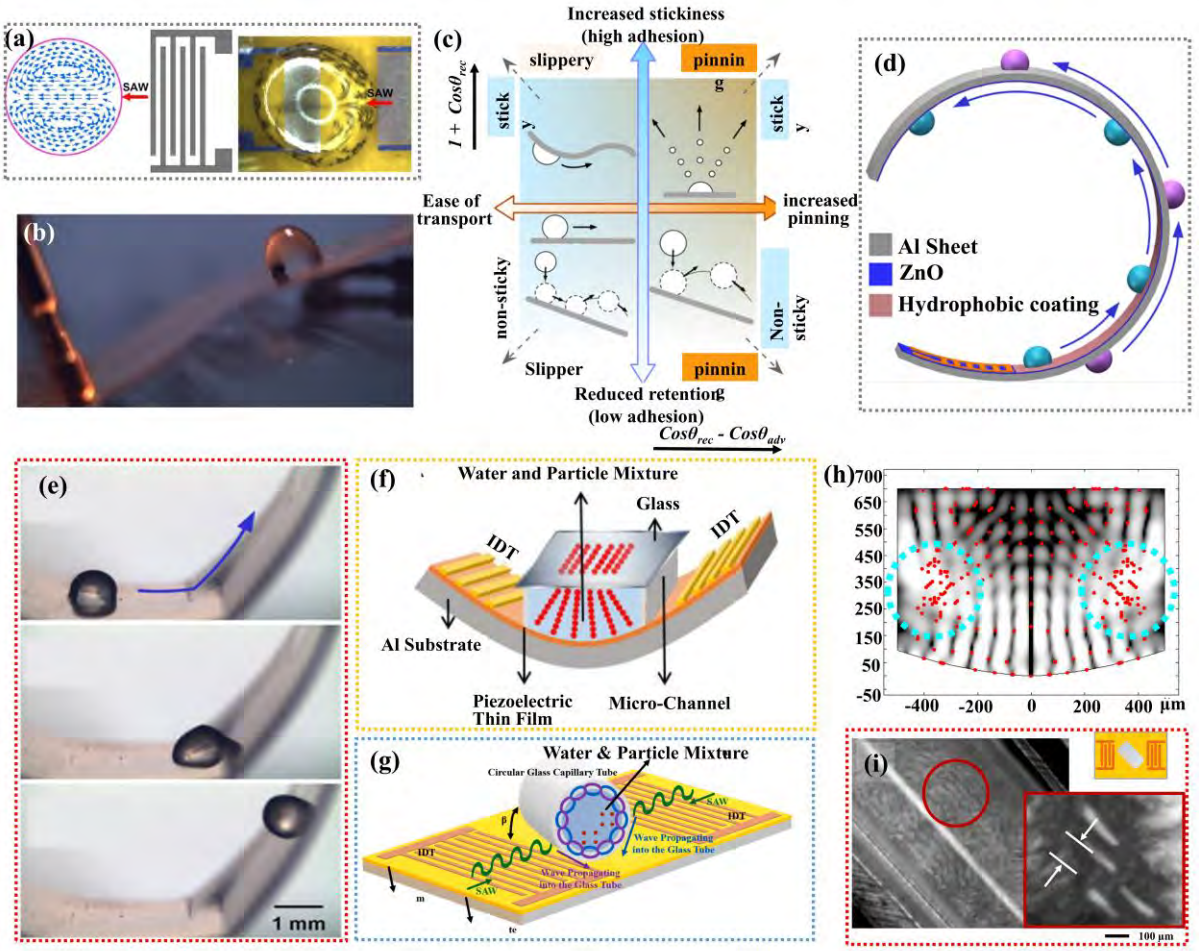

Figure.11 (a) Acoustic streaming inside the droplet, driven by flexible ZnO/PI SAW device; Reproduced with permission from Jin et al., Sci. Rep. 3, 2140 (2013). Copyright 2013 Springer Nature.[29] (b) Droplet transportation using a ZnO/Al SAW device on a 50 µm thick foil; Reproduced with permission from Liu et al., Sensor Actuat. B-Chem., 221, 230-235 (2015). Copyright Elsevier Ltd.[63] (c) Four distinctive schemes for droplet movements resulting from contact angle hysteresis and receding contact angle; Reproduced with permission from Tao et al., Nano lett. 20(5), 3263-3270 (2020). Copyright 2020 American Chemical Society.[45] (d) Schematics of droplet transport along a curved surface using a flexible 200 µm thick ZnO/Al SAW device with a hierarchical texture for efficient transport; and (e) Demonstration of droplet transportation on a curved surface using an input power of ~16 W; Reproduced with permission from Wang et al., ACS Appl. Mater. Interfaces, 13(14) 16978-16986 (2021). Copyright 2021 American Chemical Society.[30] Particle patterning in a microchamber (f) and circular glass (h) capillary tube driven by SAWs with aligned particle patterns (h, i). Reproduced with permission from Maramizonouz et al., Int. J. Mech. Sci. 214, 106893 (2022). Int. J. Mech. Sci. 202, 106536 (2021). Copyright 2021 Elsevier Ltd.[155,156]

In 2020, Tao et al. deposited the ZnO films on Al sheet/foils and proposed a new idea of

hierarchical nanotexture to promote both shear hydrophobicity and tensile hydrophilicity, thus creating nanostructured surfaces which are both slippery and sticky (**Figure 11c**), thereby enabling efficient liquid transportation on the bent SAW device surfaces.[45] They demonstrated efficient transportation of liquid droplet on inclined, vertical, inverted, or even flexible geometries using flexible ZnO/Al sheet/foil SAW devices. In 2021, Wang et al. systematically investigated acoustofluidic behaviors of ZnO/Al sheet/foil SAW devices with Al substrate thickness from 50 μm to 200 μm, and provided guidance on the design and manufacture methodology for flexible acoustofluidic devices (**Figure 11d**).[30] They found that an optimal thickness range of ~200 μm maintained efficient droplet transportation and adequate flexibility (**Figure 11e**) among the different thickness samples. When the device's bending radius is relatively small, e.g., smaller than 3 cm in their study, the microfluidic driving power was relatively high (generally >10 W). In addition, as the substrate thickness reduces, the wave mode was found to change from Rayleigh wave to hybrid wave and subsequently Lamb waves, and the microfluidic performance could be affected as it is generally agreed that Rayleigh waves should have much better acoustofluidics performance compared with those of Lamb waves.

5.2 Continuous Acoustofluidics

Acoustic wave technologies can also be used for the implementation of continuous acoustofluidics. The continuous acoustofluidics are often known as manipulation of liquids and particles in channels. Flexible continuous acoustofluidics should be designed to operate under circumstances where the surfaces are curved, inclined or even twisted. In 2021 and 2022, Maramizonouz et al. experimentally and numerically explored the flexible ZnO/Al foil SAW devices working with curved, twisted and inclined shapes for microparticles/yeast cells patterning (**Figures 11f&g**).[155,156] They found converged or diverged particle patterning lines in agreement with the bending geometry by bending the SAW devices in a concave or convex geometries. Their results showed that particles are more effectively aligned using flexural mode-based Lamb wave device, and for the SAW devices under a convex bending, the particle patterns became more regular after applying with the Rayleigh waves.

Maramizonouz et al. further investigated the influences of microchannel shape (i.e., using a capillary tube which can be wrapped by a flexible SAW device) on the cell patterns. Both simulation and experimental results showed that the standing wave fields inside the capillary tubes generated by the SAW devices were significantly determined by the geometry of the tubes, thereby leading to different patterning of particles in rectangular and circular microtubes (with examples shown in **Figures 11h&i**).[155,156] Within rectangular capillary tubes, the particles

are patterned in lines which are parallel to the side walls of microtubes. For those circular capillary tubes and along the tube's height, particles are aligned with quite different patterns. Particles are seen to be patterned into parallel lines along the tube direction at the bottom. Whereas they show patterns perpendicular to the tube direction at the middle height of the tube. Particles in a continuous liquid flow are formed patterned lines which are parallel to the flow direction under the influence of acoustic waves in both rectangular and circular glass tubes. These studies provided good solutions to one of the main challenges of continuously flexible acoustofluidics, i.e., reliable manipulation of species within the liquid phase under different bending conditions.

5.3 Potential Flexible and Wearable LOC Applications

Lab-on-a-chip (LOC) has been integrated into biology and medical research since it was first proposed in 1980s, when the development of microscale manufacture technologies and microscale devices provided the capabilities for microfluidics applications. LOC technologies enable precise manipulation of fluids at submillimeter length scale, thus enabling the realization of most bioassays with reduced sample volumes, minimized consumption of reagents, and precise control of patio-temporal dynamics,[157] showing great potentials in drug delivery, biomedical diagnostics, cell manipulation/separation, tissue engineering and organs on chip. Conventional and rigid LOC devices have been applied for biomedical assays in laboratories and hospitals. However, the emerging needs of point-of-care testing require complex or flexible assay protocols handled by less trained individuals outside professional laboratories or near the location of patients.[158] In this case, flexible LOC platforms provides merits of portability, low cost, disposability and adaptation to arbitrary surfaces.[159]

Researchers have recently developed flexible acoustic wave devices targeting highly integrated functional LOC platforms. For example, Tao et al. reported a flexible acoustic wave device implementing functionalities of both fluid handling and biomolecular sensing to realize a basic bioassay for drug detection.[160] The flexible platform, with multiple wave modes, can serve for a sequence of actuation functions, including mixing, pumping with Lamb waves and the chemotherapeutic Imatinib detection with thickness shear mode. The transportation velocity of liquid samples can reach 6 mm/s and is tunable via the input power. The monitoring of Imatinib concentration at clinical level was experimentally presented and the potential of the flexible platform was demonstrated in continuous health monitoring and disease diagnosis.

Zahertar et al. designed flexible SAW devices based on ZnO thin films coated multilayered substrates (e.g., Ni/Cu/Ni and Ni/Cu/Ni/PET) with higher flexibility by nature, and compared their acoustofluidic performance with those of ZnO/PET devices.[47] Polymer thin

films are prior substrates for flexible acoustic wave devices, yet with fatal drawbacks, such as large acoustic energy absorption, which limit their applications in LOC platforms requiring microfluidic functions. Zahertar et al. [47] solved this problem by adding a thin layer of Ni/Cu/Ni beneath the ZnO film, demonstrating acceptable performance on acoustofluidic functions of droplet actuation. The SAW devices were also applied to detect the concentration of glycerol. However, most of the attempts towards LOC are lack of fully integration with the conventional sensing system and/or bioassays, and successful demonstrations have not been made for the integrated LOC functions.

6. Summary, Challenges and Future development

6.1 Key Conclusions

In this paper, recent advances on design and fabrication of flexible SAW devices for flexible/wearable electronics and acoustofluidics LOC are discussed. They have demonstrated great promises for applications in flexible electronics such as temperature sensors, strain sensors, humidity sensors, UV sensors, chemical sensor, biosensors. They have also shown great potentials for acoustofluidics device and LOC. Considering the requirements of different sensors, different substrate materials and piezoelectric film materials or single crystalline piezoelectric film are designed. Based on the piezoelectric effect, flexible SAW temperature sensors with high stability, fast response, long service life, and wireless passive have been made. Flexible SAW strain sensors have been demonstrated with high accuracy, large sensing range, fast response and good repeatability based on the deformation effect. Based on mass loading effect, flexible SAW humidity sensors with high sensitivity, small hysteresis fast response, and real-time monitoring were shown. Based on acoustoelectric effect, flexible SAW UV sensors with good linearity, high resolution and repeatability were exploited. Besides, flexible acoustofluidics and LOC devices have been reported based on the significant wave integration with liquid medium for the flexible SAWs. Finally, the integration of wireless passive flexible SAW sensors for wearable systems is discussed.

6.2 Key Challenges and Future Opportunities

Although flexible SAW devices show numerous unique properties, they still have challenges and opportunities for future applications, which have been highlighted below.

- In order to achieve a good compatibility and conformity with the human body or skin, it is necessary to develop ultra-thin, ultra-light, stretchable and compatible flexible substrate for the SAW devices. Furthermore, it is a challenges and various methods have

been explored to manufacture high-performance (e.g., electromechanical coupling coefficient and quality factor) SAW devices on this flexible substrate, as the acoustic waves and energy are easy to attenuate in flexible substrates.

- It is difficult to prepare thick piezoelectric films with large piezoelectric coefficient and high velocity on flexible substrates, especially on many types of amorphous and flexible substrate. Material engineering such as lattice matching, high stress, and poor adhesion between films and the substrates have been the key focus in this research direction.
- It is difficult to manufacture highly miniaturized and integrated flexible SAW devices with much higher frequency for sensing (or micron or sub-micron SAW wavelengths), or devices which have high electro-mechanical coupling and high wave amplitude for acoustofluidic applications. This can be solved by selections, optimization and matching of both thin film and substrate materials.
- Ion cutting and grinding technologies for achieving high performance single crystalline piezoelectric layer for SAW devices are complex, expensive, and the utilization of bulk materials for the fabrication process is very low. The manufactured device cannot realize complex deformation and fragile. Thus, thin film processing and optimization should be the key focused technique for mass production of flexible SAW devices.
- The sensing mechanisms of various flexible SAW sensors in bending states have not been well-understood.
- How to compromise the flexibility of devices and the performance of flexible SAW sensing and microfluidics is a major problem. This will be significantly depending on material research, selections and device design and integration of flexible SAW devices.
- There is a lack of systematic research on vibration modes for sensing and microfluidic applications. The vibration mode of the wave may change in the bending state, multilayer media will lead to the complication of boundary conditions and the generation of more wave modes, strain perturbation theory of different acoustic modes need further exploration. Theoretical studies and computational simulations are urgently needed.
- Great attention should be paid to develop technologies and integrate wearable sensors with data collection, storage, or analytical devices, aiming for wearable and smart microsystems.
- New applications should be explored to widen the flexible SAW devices in robotics, health care and safety. Wearable sensing systems which can be used to detect multiple signals simultaneously should be explored.
- Combination of biocompatible materials for implantable electronics should be explored.
- Artificial intelligence technology can be integrated into the flexible SAW sensor array

and lab-on-chip, to realize the multi parameter decoupling thus make the flexible SAW system to more multifunctional, smart and accurate.

- In order to realize SAW wireless inquiry, readers usually need to transmit large transmission power, therefore, to fit for long term usages on the human body or skin, or textile surfaces with saved energy and increased sensing stability, flexible SAW devices can be integrated with wireless functions or energy harvesting devices such as triboelectric nanogenerator (TENG).

Based on the current research progress and future needs, we think there are four promising research directions in the field of flexible piezoelectric devices.

- Developing novel high-performance piezoelectric films materials (such as doped AlN or ZnO) on flexible substrate with large piezoelectric coefficient, high crystal orientation, low internal stress, and strong adhesion is essential, as improving the quality of the piezoelectric film is crucial for increasing the Q factor and enhancing performance of the flexible SAW devices. In addition, the new deposition methods for piezoelectric films should also be developed.
- To achieve the consistency for the monitoring results between the planar and curved surface configurations, it is essential to develop flexible SAW devices that are insensitive to strain, as the frequency shift of flexible SAW devices can be significantly affected by strain and mechanical deformation. A promising approach to achieve this is to propose a methodology to extract critical information from the scattering parameter of flexible SAW and combine the machine learning or artificial intelligence (AI) method to decouple multi-parameter influences and achieving anti-strain interference effects in flexible SAW sensing onto the curved surface monitoring.[161]
- Implementing a flexible SAW sensor array technology is also a promising direction that can offer several advantages over a single sensor device. A sensor array can simultaneously detect multiple analytes, enabling more comprehensive analysis of a given testing sample. This can save time and resources while improving the accuracy and sensitivity of the measurement.
- The flexible SAW sensors can achieve real-time wireless and passive monitoring, making them promising candidates for implantable devices, which can play a significant role in disease prevention and treatment. In addition, combining flexible surface acoustic wave sensors with AI enables intelligent processing and analysis of multiple parameters, bringing more accurate and reliable sensing to remote monitoring and control. These devices have great potentials for the development of intelligent wearable devices such as smartwatches, wristbands, and glasses, which can provide comprehensive health

assessments by monitoring multiple parameters such as heart rate, blood pressure, blood sugar, respiratory rate, and sleep.

Acknowledgement

This work was supported in part by the Natural Science Foundation of China (NSFC) under Grant 52075162; in part by the NSFC-Zhejiang Joint Fund for the Integration of Industrialization and information (No.U20A20172); in part by the Program of High-Tech Industry of Hunan Province under Grant 2020GK2015 and Grant 2021GK4014; in part by the Natural Science Foundation of Hunan Province under Grant 2021JJ20018; in part by the Joint Fund of the Ministry of Education (Young Talents); the Engineering Physics and Science Research Council of UK (EPSRC EP/P018998/1) and International Exchange Grant (IEC/NSFC/201078) through Royal Society UK and the NSFC.

Reference

[1] R. Su, S. Fu, Z. Lu, J. Shen, H. Xu, Z. Xu, R. Wang, C. Song, F. Zeng, and W. Wang, Appl. Phys. Lett. **120** (25), 253501 (2022).

[2] C. Sun, B. W. Soon, Y. Zhu, N. Wang, S. P. H. Loke, X. Mu, J. Tao, and A. Y. Gu, Appl. Phys. Lett. **106** (25), 253502 (2015).

[3] L. Shao, D. Zhu, M. Colangelo, D. Lee, N. Sinclair, Y. Hu, P. T. Rakich, K. Lai, K. K. Berggren, and M. Lončar, Nat. Electron., 5(6) 348 (2022).

[4] R. Sasaki, Y. Nii, and Y. Onose, Nat. Commun. **12** (1), 2599 (2021).

[5] K. J. Satzinger, Y. Zhong, H.-S. Chang, G. A. Peairs, A. Bienfait, M.-H. Chou, A. Cleland, C. R. Conner, É. Dumur, and J. Grebel, Nature **563** (7733), 661 (2018).

[6] S. Xiong, J. Zhou, J. Wu, H. Li, W. Zhao, C. He, Y. Liu, Y. Chen, Y. Fu, and H. Duan, ACS Appl. Mater. Interfaces **13** (35), 42094 (2021).

[7] M. Agostini, F. Lunardelli, M. Gagliardi, A. Miranda, L. Lamanna, A. G. Luminare, F. Gambineri, M. Lai, M. Pistello, and M. Cecchini, Adv. Funct. Mater. **32** (44), 2201958 (2022).

[8] P. Neužil, S. Giselbrecht, K. Länge, T. J. Huang, and A. Manz, Nat. Rev. Drug Discovery **11** (8), 620 (2012).

[9] Y. Kim, J. M. Suh, J. Shin, Y. Liu, H. Yeon, K. Qiao, H. S. Kum, C. Kim, H. E. Lee, C. Choi, H. Kim, D. Lee, J. Lee, J.-H. Kang, B.-I. Park, S. Kang, J. Kim, S. Kim, J. A. Perozek, K. Wang, Y. Park, K. Kishen, L. Kong, T. Palacios, J. Park, M.-C. Park, H.-J. Kim, Y. S. Lee, K. Lee, S.-H. Bae, W. Kong, J. Han, and J. Kim, Science **377** (6608), 859 (2022).

[10] A. Ozcelik, J. Rufo, F. Guo, Y. Gu, P. Li, J. Lata, and T. J. Huang, Nat. Methods **15** (12), 1021 (2018).

[11] Y. Gu, C. Chen, Z. Mao, H. Bachman, R. Becker, J. Rufo, Z. Wang, P. Zhang, J. Mai, and S. Yang, Sci. Adv. **7** (1), eabc0467 (2021).

[12] Z. Tian, S. Yang, P.-H. Huang, Z. Wang, P. Zhang, Y. Gu, H. Bachman, C. Chen, M. Wu, and Y. Xie, Sci. Adv. **5** (5), eaau6062 (2019).

[13] S. P. Zhang, J. Lata, C. Chen, J. Mai, F. Guo, Z. Tian, L. Ren, Z. Mao, P.-H. Huang, and P. Li, Nat. Commun. **9** (1), 2928 (2018).
[14] P. Zhang, C. Chen, X. Su, J. Mai, Y. Gu, Z. Tian, H. Zhu, Z. Zhong, H. Fu, and S. Yang, Sci. Adv. **6** (24), eaba0606 (2020).
[15] D. W. Branch, D. C. Hayes, and J. B. Ricken, 2020.
[16] P. Jin, J. Fu, F. Wang, Y. Zhang, P. Wang, X. Liu, Y. Jiao, H. Li, Y. Chen, and Y. Ma, Sci. Adv. **7** (40), eabg2507 (2021).
[17] Y. Chen, Z. Shu, S. Zhang, P. Zeng, H. Liang, M. Zheng and H. Duan, Int. J. Extrem. Manuf. **3**, 032002 (2021).
[18] B. Feng, H. Jin, Z. Fang, Z. Yu, S. Dong, and J. Luo, IEEE Sens. J. **21** (17), 18571 (2021).
[19] Q. Li, J. Liu, B. Yang, L. Lu, Z. Yi, Y. Tian, and J. Liu, IEEE Electron Device Lett. **40** (6), 961 (2019).
[20] J. Chen, H. Guo, X. He, W. Wang, W. Xuan, H. Jin, S. Dong, X. Wang, Y. Xu, S. Lin, S. Garner, and J. Luo, J. Micromech. Microeng. **25** (11) 115005 (2015).
[21] L. Lamanna, F. Rizzi, F. Guido, L. Algieri, S. Marras, V. M. Mastronardi, A. Qualtieri, and M. De Vittorio, Adv. Electron. Mater. **5** (6), 1900095 (2019).
[22] J. Wu, C. Yin, J. Zhou, H. Li, Y. Liu, Y. Shen, S. Garner, Y. Fu, and H. Duan, ACS Appl. Mater. Interfaces **12** (35), 39817 (2020).
[23] H. Jin, X. Tao, S. Dong, Y. Qin, L. Yu, J. Luo, and M. J. Deen, J. Micromech. Microeng. **27** (11) 115006 (2017).
[24] W. Xuan, J. Chen, X. He, W. Wang, S. Dong, and J. Luo, Procedia Eng. **120**, 364 (2015).
[25] C. Yin, J. Wu, J. Zhou, D. Zhang, Z. Liu, X. Liu, L. Liu, Z. Zhan, S. Garner, and Y. Fu, Sens. Actuators, A **321** 112590 (2021).
[26] Y. Kim, J. M. Suh, J. Shin, Y. Liu, H. Yeon, K. Qiao, H. S. Kum, C. Kim, H. E. Lee, and C. Choi, Science **377** (6608), 859 (2022).
[27] L. Lamanna, F. Rizzi, V. R. Bhethanabotla, and M. De Vittorio, Biosens. Bioelectron. **163** 112164 (2020).
[28] L. Piro, L. Lamanna, F. Guido, A. Balena, M. Mariello, F. Rizzi, and M. De Vittorio, Nanomaterials **11** (6), 1479 (2021).
[29] H. Jin, J. Zhou, X. He, W. Wang, H. Guo, S. Dong, D. Wang, Y. Xu, J. Geng, J. K. Luo, and W. I. Milne, Sci. Rep. **3** 1 (2013).
[30] Y. Wang, Q. Zhang, R. Tao, J. Xie, P. Canyelles-Pericas, H. Torun, J. Reboud, G. McHale, L. E. Dodd, and X. Yang, ACS Appl. Mater. Interfaces **13** (14), 16978 (2021).
[31] C. Sun, R. Mikhaylov, Y. Fu, F. Wu, H. Wang, X. Yuan, Z. Xie, D. Liang, Z. Wu, and X. Yang, IEEE Trans. Electron Devices **68** (1), 393 (2020).
[32] C.-H. Zhang, Y. Yang, C.-J. Zhou, Y. Shu, H. Tian, Z. Wang, Q.-T. Xue, and T.-L. Ren, Chin. Phys. Lett. **30** (7), 077701 (2013).
[33] Z. Ji, J. Zhou, H. Lin, J. Wu, D. Zhang, S. Garner, A. Gu, S. Dong, Y. Fu, and H. Duan, Microsyst. Nanoeng. **7**, 97 (2021).
[34] X. He, H. Guo, J. Chen, W. Wang, W. Xuan, Y. Xu, and J. Luo, Appl. Phys. Lett. **104** (21) 213504 (2014).
[35] Y. Q. Fu, J. K. Luo, N. T. Nguyen, A. J. Walton, A. J. Flewitt, X. T. Zu, Y. Li, G. McHale, A. Matthews, E. Iborra, H. Du, and W. I. Milne, Prog. Mater Sci. **89**, 31 (2017).

[36] J. Zhou, X. He, H. Jin, W. Wang, B. Feng, S. Dong, D. Wang, G. Zou, and J. Luo, J. Appl. Phys. **114** (4), 044502 (2013).
[37] H. Jin, J. Zhou, S. Dong, B. Feng, J. Luo, D. Wang, W. Milne, and C. Y. Yang, Thin Solid Films **520** (15), 4863 (2012).
[38] H. Xu, S. Dong, W. Xuan, U. Farooq, S. Huang, M. Li, T. Wu, H. Jin, X. Wang, and J. Luo, Appl. Phys. Lett. **112** (9) 093502 (2018).
[39] C. Deus, J. Salomon, and U. Wehner, Vak. Forsch. Prax. **28** (4), 40 (2016).
[40] J. K. Chen, X. L. He, W. B. Wang, W. P. Xuan, J. Zhou, X. Z. Wang, S. R. Dong, S. Garner, P. Cimo, and J. K. Luo, J. Mater. Chem. C **2** (43), 9109 (2014).
[41] A. Plichta, A. Weber, and A. Habeck, MRS Online Proc. Libr. **769** (2003).
[42] W. S. Wong and A. Salleo, *Flexible electronics: materials and applications*. (Springer Science & Business Media, 2009).
[43] C. Wang, C. Linghu, S. Nie, C. Li, Q. Lei, X. Tao, Y. Zeng, Y. Du, S. Zhang, K. Yu, H. Jin, W. Chen, and J. Song, Sci Adv **6** (25), eabb2393 (2020).
[44] X. L. He, J. Zhou, W. B. Wang, W. P. Xuan, X. Yang, H. Jin, and J. K. Luo, J. Micromech. Microeng. **24** (5) (2014).
[45] R. Tao, G. McHale, J. Reboud, J. M. Cooper, H. Torun, J. Luo, J. Luo, X. Yang, J. Zhou, P. Canyelles-Pericas, Q. Wu, and Y. Fu, Nano Lett. **20** (5), 3263 (2020).
[46] R. Tao, S. Zahertar, H. Torun, Y. R. Liu, M. Wang, Y. Lu, J. T. Luo, J. Vernon, R. Binns, Y. He, K. Tao, Q. Wu, H. L. Chang, and Y. Q. Fu, ACS Sensors **5** (8), 2563 (2020).
[47] S. Zahertar, R. Tao, H. Wang, H. Torun, P. Canyelles-Pericas, Y. Liu, J. Vernon, W. P. Ng, R. Binns, Q. Wu, J. Luo, and Y.-Q. Fu, IEEE Sens. J. 1 (2022).
[48] W. A. MacDonald, J. Mater. Chem. **14** (1), 4 (2004).
[49] I. C. Cheng, A. Kattamis, K. Long, J. C. Sturm, and S. Wagner, J. Soc. Inf. Disp. **13** (7), 563 (2005).
[50] S. Khan, L. Lorenzelli, and R. S. Dahiya, IEEE Sens. J. **15** (6), 3164 (2015).
[51] W. A. MacDonald, in *Large Area and Flexible Electronics* (2015), pp. 291.
[52] V. Zardetto, T. M. Brown, A. Reale, and A. Di Carlo, J. Polym. Sci., Part B: Polym. Phys. **49** (9), 638 (2011).
[53] Y. Jouane, S. Colis, G. Schmerber, A. Dinia, P. Lévêque, T. Heiser, and Y.-A. Chapuis, Org. Electron. **14** (7), 1861 (2013).
[54] S. R. Heron, R. Wilson, S. A. Shaffer, D. R. Goodlett, and J. M. Cooper, Anal. Chem. **82** (10), 3985 (2010).
[55] J. Shi, D. Ahmed, X. Mao, S.-C. S. Lin, A. Lawit, and T. J. Huang, Lab Chip **9** (20), 2890 (2009).
[56] X. Du, Y. Q. Fu, S. Tan, J. Luo, A. Flewitt, W. Milne, D.-S. Lee, N.-M. Park, J. Park, and Y. Choi, Appl. Phys. Lett. **93** (9), 094105 (2008).
[57] P. Muralt, J. Am. Ceram. Soc. **91** (5), 1385 (2008).
[58] Ü. Özgür, D. Hofstetter, and H. Morkoc, Proc. IEEE **98** (7), 1255 (2010).
[59] M. Willander, O. Nur, Q. Zhao, L. Yang, M. Lorenz, B. Cao, J. Z. Pérez, C. Czekalla, G. Zimmermann, and M. Grundmann, Nanotechnology **20** (33), 332001 (2009).
[60] Y. Yoshino, J. Appl. Phys. **105** (6), 061623 (2009).
[61] L. Fan, S.-y. Zhang, H. Ge, and H. Zhang, J. Appl. Phys. **114** (2), 024504 (2013).
[62] X. He, D. Li, J. Zhou, W. Wang, W. Xuan, S. Dong, H. Jin, and J. Luo, J. Mater. Chem.

C **1** (39), 6210 (2013).
[63] Y. Liu, Y. Li, A. M. el-Hady, C. Zhao, J. F. Du, Y. Liu, and Y. Q. Fu, Sens. Actuators, B **221**, 230 (2015).
[64] Y. Liu, J. T. Luo, C. Zhao, J. Zhou, S. A. Hasan, Y. Li, M. Cooke, Q. Wu, W. P. Ng, and J. F. Du, IEEE Trans. Electron Devices **63** (11), 4535 (2016).
[65] A. Muller, G. Konstantinidis, D. Neculoiu, A. Dinescu, C. Morosanu, A. Stavrinidis, M. Dragoman, D. Vasilache, C. Buiculescu, and I. Petrini, presented at the 2008 Asia-Pacific Microwave Conference, 2008 (unpublished).
[66] S. Xiong, X. Liu, J. Zhou, Y. Liu, Y. Shen, X. Yin, J. Wu, R. Tao, Y. Fu, and H. Duan, RSC Adv. **10** (33), 19178 (2020).
[67] J. Zhou, S. Dong, H. Jin, B. Feng, and D. Wang, J. Control Sci. Eng. **2012** (2012).
[68] K. Li, F. Wang, M. Deng, K. Hu, D. Song, Y. Hao, H. Di, K. Dong, S. Yan, and Z. Song, J. Mater. Sci.: Mater. Electron. **32** (10), 13146 (2021).
[69] J.-B. Lee, D.-H. Cho, D.-Y. Kim, C.-K. Park, and J.-S. Park, Thin Solid Films **516** (2), 475 (2007).
[70] J. Ji, F. Liu, N. A. Hashim, M. M. Abed, and K. Li, React. Funct. Polym. **86**, 134 (2015).
[71] A. Jain, P. K. J, A. K. Sharma, A. Jain, and R. P.N, Polym. Eng. Sci. **55** (7), 1589 (2015).
[72] Y. Kubouchi, Y. Kometani, T. Yagi, T. Masuda, and A. Nakajima, Pure Appl. Chem. **61** (1), 83 (1989).
[73] J. A. Grubb, Electrocomponent Sci. Technol. **9**, 972816 (1982).
[74] R. S. C. Monkhouse, P. D. Wilcox, and P. Cawley, Ultrasonics **35** (7), 489 (1997).
[75] D. M. G. Preethichandra and K. Kaneto, IEEE Sens. J. **7** (5), 646 (2007).
[76] B. Zivasatienraj, M. B. Tellekamp, and W. A. Doolittle, Crystals **11** (4), 397 (2021).
[77] P. Meek, L. Holland, and P. Townsend, Thin Solid Films **141** (2), 251 (1986).
[78] T. Kanata, Y. Kobayashi, and K. Kubota, J. Appl. Phys. **62** (7), 2989 (1987).
[79] T. A. Rost, R. C. Baumann, B. A. Stone, and T. A. Rabson, presented at the [Proceedings] 1990 IEEE 7th International Symposium on Applications of Ferroelectrics, 1990 (unpublished).
[80] N. Fujimura, T. Ito, and M. Kakinoki, J. Cryst. Growth **115** (1-4), 821 (1991).
[81] T. A. Rost, H. Lin, T. A. Rabson, R. C. Baumann, and D. L. Callahan, J. Appl. Phys. **72** (9), 4336 (1992).
[82] M. Shimizu, Y. Furushima, T. N. T. Nishida, and T. S. T. Shiosaki, Jpn. J. Appl. Phys. **32** (9S), 4111 (1993).
[83] G. Poberaj, M. Koechlin, F. Sulser, A. Guarino, J. Hajfler, and P. Gunter, Opt. Mater. **31** (7), 1054 (2009).
[84] Y. Osugi, T. Yoshino, K. Suzuki, T. Hirai, and Ieee, presented at the IEEE/MTT-S International Microwave Symposium, Honolulu, HI, 2007 (unpublished).
[85] S. Zhang, R. Lu, H. Zhou, S. Link, Y. Yang, Z. Li, K. Huang, X. Ou, and S. Gong, IEEE Trans. Microwave Theory Tech. **68** (9), 3653 (2020).
[86] C. Floer, S. Hage-Ali, L. Verzellesi, L. Badie, O. Elmazria, and S. Zhgoon, presented at the 2019 IEEE SENSORS, 2019 (unpublished).
[87] G. Poberaj, H. Hu, W. Sohler, and P. Günter, Laser Photonics Rev. **6** (4), 488 (2012).
[88] S. Gupta, W. T. Navaraj, L. Lorenzelli, and R. Dahiya, npj Flexible Electron. **2** (1) (2018).

[89] H. Xu, Z. Cao, S. Dong, J. Chen, W. Xuan, W. Cheng, S. Huang, L. Shi, S. Liu, U. Farooq, A. Qadir, and J. Luo, J. Micromech. Microeng. **29** (2), 025003 (2018).
[90] A. L. Nalamwar and M. Epstein, J. Appl. Phys. **47** (1), 43 (1976).
[91] B. A. Auld, *Acoustic fields and waves in solids*. (Рипол Классик, 1973).
[92] R. Tao, W. Wang, J. Luo, S. A. Hasan, H. Torun, P. Canyelles-Pericas, J. Zhou, W. Xuan, M. Cooke, and D. Gibson, Surf. Coat. Technol. **357**, 587 (2019).
[93] K. Sezawa and K. Kanai, Proc. Imp. Acad. **11** (1), 13 (1935).
[94] N. Barie and M. Rapp, Biosens. Bioelectron. **16** (9-12), 979 (2001).
[95] G. Kovacs and A. Venema, Appl. Phys. Lett. **61** (6), 639 (1992).
[96] J. W. Grate, S. W. Wenzel, and R. M. White, Anal. Chem. **63** (15), 1552 (1991).
[97] R. Tao, S. A. Hasan, H. Z. Wang, J. Zhou, J. T. Luo, G. McHale, D. Gibson, P. Canyelles-Pericas, M. D. Cooke, and D. Wood, Sci. Rep. **8** (1), 1 (2018).
[98] R. Tao, S. A. Hasan, H. Z. Wang, J. Zhou, J. T. Luo, G. McHale, D. Gibson, P. Canyelles-Pericas, M. D. Cooke, D. Wood, Y. Liu, Q. Wu, W. P. Ng, T. Franke, and Y. Q. Fu, Sci. Rep. **8** (2018).
[99] J. Zhou, Z. Ji, Y. Guo, Y. Liu, F. Zhuo, Y. Zheng, Y. A. Gu, Y. Fu, and H. Duan, npj Flexible Electron. **6** (1), 1 (2022).
[100] A. l. Nalamwar and M. Epstein, IEEE Transactions on Sonics and Ultrasonics. **23**, 144 (1976).
[101] J. Zhou, Z. Ji, Y. Guo, Y. Liu, F. Zhuo, Y. Zheng, Y. Gu, Y. Fu, and H. Duan, npj Flexible Electron. **6** (1), 84 (2022).
[102] Q. Zhang, Y. Wang, D. Li, X. Yang, J. Xie, and Y. Fu, Appl. Phys. Lett. **118** (12), 121601 (2021).
[103] S. Rokhlin and L. Wang, J, Acoust. Soc. Am. **112** (3), 822 (2002).
[104] M. Hoummady, A. Campitelli, and W. Wlodarski, Smart Mater. Struct. **6** (6), 647 (1997).
[105] D. Rebière, G. Duchamp, J. Pistré, M. Hoummady, D. Hauden, and R. Planade, Sens. Actuators, B **14** (1-3), 642 (1993).
[106] D. Rebière, J. Pistré, M. Hoummady, D. Hauden, P. Cunin, and R. Planade, Sens. Actuators, B **6** (1-3), 274 (1992).
[107] A. Mujahid and F. L. Dickert, Sensors (Basel) **17** (12), 2716 (2017).
[108] G. Panneerselvam, V. Thirumal, and H. M. Pandya, Arch. Acoust. **43** (3), 357 (2018).
[109] Y. Huang, P. K. Das, and V. R. Bhethanabotla, Sens. Actuators Rep. **3** (2021).
[110] D. Mandal and S. Banerjee, Sensors (Basel) **22** (3) (2022).
[111] T. M. A. Gronewold, Anal. Chim. Acta **603** (2), 119 (2007).
[112] B. Q. Liu, T. Han, and C. R. Zhang, IEEE Sens. J. **15** (6), 3608 (2015).
[113] J. Bardong, T. Aubert, N. Naumenko, G. Bruckner, S. Salzmann, and L. M. Reindl, IEEE Trans. Sonics Ultrason. **60** (4), 814 (2013).
[114] S. Kim, H. Wang, I. Park, and K. Lee, IEEE Sens. J. **21** (18), 19863 (2021).
[115] B. Arman Kuzubasoglu and S. Kursun Bahadir, Sens. Actuators, A **315** (2020).
[116] Y. Guo, J. Zhou, Z. Ji, Y. Liu, R. Cao, F. Zhuo, K. Tan, H. Duan, and Y. Fu, Microsyst. Nanoeng. **8** (1) (2022).
[117] Y. Wang, Y. Luo, and L. Qiu, IEEE Sens. J. **20** (1), 102 (2020).
[118] L. Li, B. Peng, J. Zhu, Z. He, Y. Yang, and W. Zhang, IEEE Sens. J. **21** (4), 4688 (2021).

[119] S. F. Jilani, D. Leff, A. Maskay, R. J. Lad, M. P. da Cunha, and Ieee, presented at the IEEE International Ultrasonics Symposium (IEEE IUS), Las Vegas, NV, 2020 (unpublished).
[120] V. Kalinin, A. Leigh, A. Stopps, and Ieee, presented at the 30th European Frequency and Time Forum (EFTF), Univ York, York, ENGLAND, 2016 (unpublished).
[121] L. Shu, X. Wang, L. Li, D. Yan, L. Peng, L. Fan, and W. Wu, Sens. Actuators, A **293**, 14 (2019).
[122] L. Lamanna, F. Rizzi, F. Giudo, and M. D. Vittorio, IEEE Electron Device Lett. **41** (11), 1692 (2020).
[123] Z. Chen and C. Lu, Sens. Lett. **3** (4), 274 (2005).
[124] T. A. Blank, L. P. Eksperiandova, and K. N. Belikov, Sens. Actuators, B **228**, 416 (2016).
[125] X. Tao, H. Jin, M. Mintken, N. Wolff, Y. Wang, R. Tao, Y. Li, H. Torun, J. Xie, J. Luo, J. Zhou, Q. Wu, S. Dong, J. Luo, L. Kienle, R. Adelung, Y. K. Mishra, and Y. Q. Fu, ACS Appl. Nano Mater. **3** (2), 1468 (2020).
[126] Y. Zhang, Y. Cai, J. Zhou, Y. Xie, Q. W. Xu, Y. Zou, S. S. Guo, H. X. Xu, C. L. Sun, and S. Liu, Sci. Bull. **65** (7), 587 (2020).
[127] S. A. Hasan, D. Gibson, M. D. Cooke, H. Torun, Q. Wu, and Y. Fu, presented at the IEEE Jordan International Joint Conference on Electrical Engineering and Information Technology (JEEIT), Amman, JORDAN, 2019 (unpublished).
[128] A. Janotti and C. G. Van de Walle, Rep. Prog. Phys. **72** (12), 126501 (2009).
[129] V. Chivukula, D. Ciplys, M. Shur, and P. Dutta, Appl. Phys. Lett. **96** (23), 233512 (2010).
[130] H. Chen, L. Su, M. Jiang, and X. Fang, Adv. Funct. Mater. **27** (45), 1704181 (2017).
[131] Q. Zhang, Y. Wang, R. Tao, H. Torun, J. Xie, Y. Li, C. Fu, J. Luo, Q. Wu, and W. P. Ng, J. Micromech. Microeng. **30** (9), 095010 (2020).
[132] Q. Zhang, Y. Wang, T. Wang, D. Li, J. Xie, H. Torun, and Y. Fu, ACS Sens. **6** (8), 3072 (2021).
[133] Y. Wang, X. Tao, R. Tao, J. Zhou, Q. Zhang, D. Chen, H. Jin, S. Dong, J. Xie, and Y. Q. Fu, Sens. Actuators, A **306**, 111967 (2020).
[134] L. Y. Yeo and J. R. Friend, Annu. Rev. Fluid Mech **46** (1), 379 (2014).
[135] J. H. Jung, G. Destgeer, J. Park, H. Ahmed, K. Park, and H. J. Sung, RSC Adv. **8** (6), 3206 (2018).
[136] W. Liang and G. Lindner, J. Appl. Phys. **114** (4), 044501 (2013).
[137] M. Zhang, J. Huang, Y. Lu, W. Pang, H. Zhang, and X. Duan, ACS Sens. **3** (8), 1584 (2018).
[138] Y. Lu, M. Zhang, H. Zhang, J. Huang, Z. Wang, Z. Yun, Y. Wang, W. Pang, X. Duan, and H. Zhang, Microfluid. Nanofluid. **22** (12), 1 (2018).
[139] S. Shiokawa, Y. Matsui, and T. Moriizumi, Jpn. J. Appl. Phys. **28** (S1), 126 (1989).
[140] L. Y. Yeo and J. R. Friend, Biomicrofluidics **3** (1), 012002 (2009).
[141] J. Zhou, M. DeMiguel-Ramos, L. Garcia-Gancedo, E. Iborra, J. Olivares, H. Jin, J. Luo, A. Elhady, S. Dong, and D. Wang, Sens. Actuators, B **202**, 984 (2014).
[142] X. Tao, T. Dai Nguyen, H. Jin, R. Tao, J. Luo, X. Yang, H. Torun, J. Zhou, S. Huang, and L. Shi, Sens. Actuators, B **299**, 126991 (2019).

[143] M. Wu, Y. Ouyang, Z. Wang, R. Zhang, P.-H. Huang, C. Chen, H. Li, P. Li, D. Quinn, and M. Dao, Proceedings of the National Academy of Sciences **114** (40), 10584 (2017).
[144] M. Wu, A. Ozcelik, J. Rufo, Z. Wang, R. Fang, and T. Jun Huang, Microsyst. Nanoeng. **5** (1), 1 (2019).
[145] R. Shilton, M. K. Tan, L. Y. Yeo, and J. R. Friend, J. Appl. Phys. **104** (1), 014910 (2008).
[146] F. Guo, Z. Mao, Y. Chen, Z. Xie, J. P. Lata, P. Li, L. Ren, J. Liu, J. Yang, and M. Dao, Proceedings of the National Academy of Sciences **113** (6), 1522 (2016).
[147] D. Ahmed, A. Ozcelik, N. Bojanala, N. Nama, A. Upadhyay, Y. Chen, W. Hanna-Rose, and T. J. Huang, Nat. Commun. **7** (1), 12150 (2016).
[148] J. Rufo, F. Cai, J. Friend, M. Wiklund, and T. J. Huang, Nat. Rev. Methods Primers **2** (1), 30 (2022).
[149] W. Wang, X. He, J. Zhou, H. Gu, W. Xuan, J. Chen, X. Wang, and J. Luo, J. Electrochem. Soc. **161** (10), B230 (2014).
[150] Y. Wang, R. Tao, Q. Zhang, D. Chen, L. Yang, W. Huang, J. Xie, and Y. Fu, presented at the 2020 IEEE 33rd International Conference on Micro Electro Mechanical Systems (MEMS), 2020 (unpublished).
[151] J. Zhou, X. Tao, J. Luo, Y. Li, H. Jin, S. Dong, J. Luo, H. Duan, and Y. Fu, Surf. Coat. Technol. **367**, 127 (2019).
[152] J. Zhou, H.-F. Pang, L. Garcia-Gancedo, E. Iborra, M. Clement, D. Miguel-Ramos, H. Jin, J. Luo, S. Smith, and S. Dong, Microfluid. Nanofluid. **18** (4), 537 (2015).
[153] Y. Wang, Q. Zhang, R. Tao, D. Chen, J. Xie, H. Torun, L. E. Dodd, J. Luo, C. Fu, and J. Vernon, Sens. Actuators, A **318**, 112508 (2021).
[154] X. Zhou, C. Zhao, R. Hou, J. Zhang, K. Kirk, D. Hutson, Y. Guo, P. A. Hu, S. Peng, and X.-T. Zu, Ultrasonics **54** (7), 1991 (2014).
[155] S. Maramizonouz, C. Jia, M. Rahmati, T. Zheng, Q. Liu, H. Torun, Q. Wu, and Y. Fu, Int. J. Mech. Sci. **214**, 106893 (2022).
[156] S. Maramizonouz, X. Tao, M. Rahmati, C. Jia, R. Tao, H. Torun, T. Zheng, H. Jin, S. Dong, and J. Luo, Int. J. Mech. Sci. **202**, 106536 (2021).
[157] E. K. Sackmann, A. L. Fulton, and D. J. Beebe, Nature **507** (7491), 181 (2014).
[158] M. Yang, Y. Liu, and X. Jiang, Chem. Soc. Rev. **48** (3), 850 (2019).
[159] A. Economou, C. Kokkinos, and M. Prodromidis, Lab Chip **18** (13), 1812 (2018).
[160] R. Tao, J. Reboud, H. Torun, G. McHale, L. E. Dodd, Q. Wu, K. Tao, X. Yang, J. T. Luo, and S. Todryk, Lab Chip **20** (5), 1002 (2020).
[161] K. Tan, Z. Ji, J. Zhou, Z. Deng, S. Zhang, Y. Gu, Y. Guo, F. Zhuo, H. Duan, and Y. Fu, Appl. Phys. Lett. **122** (1), 014101 (2023).